Science of the Total Environment 813 (2022) 152281

Contents lists available at ScienceDirect

Science of the Total Environment

journal homepage: www.elsevier.com/locate/scitotenv

The unknown third – Hydrogen isotopes in tree-ring cellulose across Europe

V. Vitali [a,*], E. Martínez-Sancho [b], K. Treydte [b], L. Andreu-Hayles [c,d,e], I. Dorado-Liñán [f], E. Gutierrez [g], G. Helle [h], M. Leuenberger [i], N.J. Loader [j], K.T. Rinne-Garmston [k], G.H. Schleser [l], S. Allen [m], J.S. Waterhouse [n], M. Saurer [a,1], M.M. Lehmann [a,1]

[a] Stable Isotope Research Center (SIRC), Ecosystem Ecology, Forest Dynamics, Swiss Federal Institute for Forest, Snow and Landscape Research WSL, Forest Dynamics, CH-8903 Birmensdorf, Switzerland
[b] Dendrosciences, Forest Dynamics, Swiss Federal Institute for Forest, Snow and Landscape Research WSL, Forest Dynamics, CH-8903 Birmensdorf, Switzerland
[c] Tree-Ring Laboratory, Lamont–Doherty Earth Observatory of Columbia University, Palisades, NY, USA
[d] CREAF, Bellaterra (Cerdanyola del Vall.s), Barcelona, Spain
[e] ICREA, Pg. Lluís Companys 23, Barcelona, Spain
[f] Department of Systems and Natural Resources, Universidad Politécnica de Madrid, Madrid, Spain.
[g] Departament de Biologia Evolutiva, Ecologia i Ciències Ambientals, Universitat de Barcelona, Barcelona, Spain
[h] German Research Centre for Geosciences, Section 4.3 Climate Dynamics and Landscape Evolution, Telegrafenberg, 14473 Potsdam, Germany
[i] Climate and Environmental Physics Division and Oeschger Centre for Climate Change Research, University of Bern, Sidlerstrasse 5, 3012 Bern, Switzerland
[j] Department of Geography, Swansea University, Swansea, UK
[k] Natural Resources Institute Finland (Luke), Helsinki, Finland
[l] FZJ Research Center Jülich, Institute of Bio- and Geosciences, Agrosphere (IBG-3), 52425 Jülich, Germany
[m] Department of Natural Resources and Environmental Science, University of Nevada Reno, 1664 N Virginia St., Reno, NV 89557, USA
[n] School of Life Sciences, Anglia Ruskin University, Cambridge, UK

HIGHLIGHTS

- The climate information in hydrogen isotope ratios of tree rings (δ^2H_c) is uncertain.
- We present the first European-wide century-long study of δ^2H_c.
- δ^2H_c is a weaker climate proxy compared to $\delta^{13}C_c$ and $\delta^{18}O_c$.
- The climate δ^2H_c signal is stronger for *Pinus* than for *Quercus*.
- δ^2H_c records a mixture of hydrological, climatic, and physiological signals.

GRAPHICAL ABSTRACT

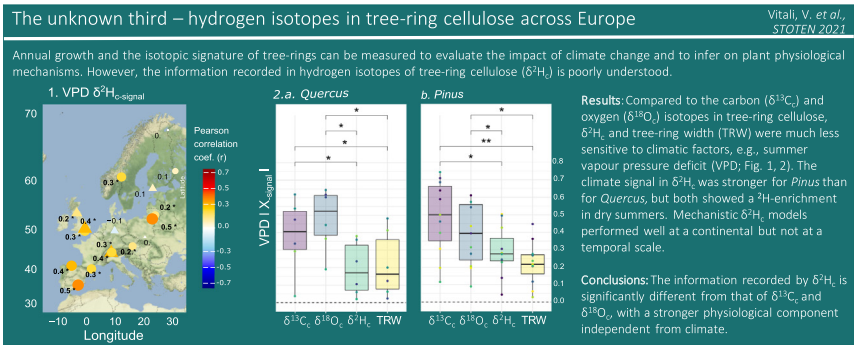

ARTICLE INFO

Article history:
Received 8 September 2021
Received in revised form 24 November 2021
Accepted 5 December 2021
Available online 21 December 2021

Editor: Christian Herrera

ABSTRACT

This is the first Europe-wide comprehensive assessment of the climatological and physiological information recorded by hydrogen isotope ratios in tree-ring cellulose (δ^2H_c) based on a unique collection of annually resolved 100-year tree-ring records of two genera (*Pinus* and *Quercus*) from 17 sites (36°N to 68°N). We observed that the high-frequency climate signals in the δ^2H_c chronologies were weaker than those recorded in carbon ($\delta^{13}C_c$) and oxygen isotope signals ($\delta^{18}O_c$) but similar to the tree-ring width ones (TRW). The δ^2H_c climate signal strength varied across the continent and was stronger and more consistent for *Pinus* than for *Quercus*. For both genera, years with extremely dry summer conditions caused a significant ^2H-enrichment in tree-ring cellulose.

* Corresponding author.
E-mail address: valentina.vitali@wsl.ch (V. Vitali).
[1] Joint senior author.

http://dx.doi.org/10.1016/j.scitotenv.2021.152281

Keywords:
Climate change
Dendroecology
Deuterium
European forests
Isotope fractionation
Mechanistic modelling
Stable isotopes
Tree physiology

The δ^2H_c inter-annual variability was strongly site-specific, as a result of the imprinting of climate and hydrology, but also physiological mechanisms and tree growth. To differentiate between environmental and physiological signals in δ^2H_c, we investigated its relationships with $\delta^{18}O_c$ and TRW. We found significant negative relationships between δ^2H_c and TRW (7 sites), and positive ones between δ^2H_c and $\delta^{18}O_c$ (10 sites). The strength of these relationships was nonlinearly related to temperature and precipitation. Mechanistic δ^2H_c models performed well for both genera at continental scale simulating average values, but they failed on capturing year-to-year δ^2H_c variations. Our results suggest that the information recorded by δ^2H_c is significantly different from that of $\delta^{18}O_c$, and has a stronger physiological component independent from climate, possibly related to the use of carbohydrate reserves for growth. Advancements in the understanding of ^2H-fractionations and their relationships with climate, physiology, and species-specific traits are needed to improve the modelling and interpretation accuracy of δ^2H_c. Such advancements could lead to new insights into trees' carbon allocation mechanisms, and responses to abiotic and biotic stress conditions.

1. Introduction

Tree-ring cellulose chronologies of stable carbon ($\delta^{13}C_c$) and oxygen ($\delta^{18}O_c$) isotopes, together with tree-ring width (TRW), have been used extensively to investigate the effects of past climatic conditions on tree growth (e.g. Andreu-Hayles et al., 2017; Barbour et al., 2002; Loader et al., 2007; Loader et al., 2020; Saurer et al., 1995; Saurer et al., 1997a; Shestakova and Martínez-Sancho, 2021) and physiological performance (e.g. Andreu-Hayles et al., 2011; Frank et al., 2015; Guerrieri et al., 2019; Klesse et al., 2018; Levesque et al., 2019; Martínez-Sancho et al., 2018). In particular, $\delta^{13}C_c$ and $\delta^{18}O_c$ have been recognized as strong continental-scale climate proxies for long-term trends in the ISONET network (Loader et al., 2013; Saurer et al., 2014; Shestakova et al., 2019; Treydte et al., 2007), as well as in the high-frequency in other European-scale studies (Vitali et al., 2021). In contrast, the environmental, climatic, and physiological information recorded by the third component of tree-ring cellulose $(C_6H_{10}O_5)_n$, the non-exchangeable carbon-bound hydrogen (δ^2H_c), has been investigated far less. Some studies on δ^2H_c and its relationship with climate have been conducted for single sites (Etien et al., 2009; Hafner et al., 2011; Haupt et al., 2011; Hilasvuori and Berninger, 2010; Lipp et al., 1991; Loader et al., 2008; Szczepanek et al., 2006), while continental-scale assessments of δ^2H_c are few (Nakatsuka et al., 2020a; Voelker et al., 2014) and still lacking in Europe. The usability and interpretation of δ^2H_c chronologies has improved recently as a result of methodological developments that have increased sample processing power (Filot et al., 2006; Sauer et al., 2009), thus advancing knowledge on how ^2H-fractionation processes relate to physiology and biochemical pathways (Cormier et al., 2018; Sanchez-Bragado et al., 2019) and expanding δ^2H analysis to various plant compounds (e.g. lipids and lignin: (Anhäuser et al., 2020; Gori et al., 2013; Riechelmann et al., 2017; Sachse et al., 2012)). These new advancements can facilitate the use of δ^2H_c in ecological research; however, further knowledge on the fundamental drivers and spatiotemporal patterns of δ^2H_c is needed to guide the interpretation of δ^2H_c variability.

Previous research has revealed uncertainties regarding the climate information that can be inferred from δ^2H_c chronologies (Boettger et al., 2014; Loader et al., 2008; Pendall, 2000; Waterhouse et al., 2002). While consistent temperature signals in δ^2H_c were observed in some earlier studies (Feng and Epstein, 1994; Gray and Song, 1984), more recent studies led to additional interpretations of the factors driving differences between sites and species. In Poland, strong correlations of δ^2H_c with summer temperature were found for *Quercus*, and with summer precipitation and winter temperature for *Pinus* (Szczepanek et al., 2006). In Austria, a *Quercus* δ^2H_c chronology reflected both summer relative humidity and temperature (Haupt et al., 2011). In Finland, at the northernmost limit of *Quercus*' European distribution, precipitation and relative humidity, but not temperature, showed a strong correlation with δ^2H_c (Hilasvuori and Berninger, 2010). These apparently contrasting results suggest that the climate signal stored in δ^2H_c tree-ring chronologies is driven by a complex interaction between climatic and environmental processes that varies across geographic regions (Lehmann et al., 2021b) and is amended by species-specific differences (Arosio et al., 2020b). Controlled experiments support the hypothesis that physiological differences among plant species interfere with δ^2H_c climate signals, as demonstrated by the tight coupling between a plant's metabolism, ^2H-fractionations, and the resulting δ^2H values (Cormier et al., 2018; Sanchez-Bragado et al., 2019). A recent study suggested that δ^2H_c record the use of old carbohydrate reserves versus fresh photosynthates for wood formation (Lehmann et al., 2021b). These findings indicate to the potential of δ^2H_c chronologies as physiological proxies for carbon allocation processes that are not captured by other tree-ring parameters.

To make full use of the information captured in δ^2H_c records, a better understanding of the ^2H-fractionation pathways, from the uptake of H_2O from the soil and CO_2 from the atmosphere to cellulose formation, and the influence of environmental conditions and tree internal processes is needed. The hydrogen isotopic composition of environmental water (e.g. precipitation, soil water, and atmospheric water vapour) is closely linked to and reflects the primary factors affecting δ^2H_c variation (Craig, 1961; Joussaume and Jouzel, 1993). Soil can contain water that reflects isotope ratios from several previous precipitation events, resulting in soil water isotope ratios potentially deviating considerably from annual precipitation (Allen et al., 2019). At the soil–tree interface, it is often claimed that no isotope fractionation occurs during root water uptake and transport (White et al., 1985), although an unexpected ^2H-fractionation effect was recently observed at the root level (Barbeta et al., 2020). At the leaf level, strong isotopic fractionation is induced by leaf and twig evapotranspiration (Cernusak et al., 2016; Treydte et al., 2014), and by the mixing with atmospheric water vapour (Lehmann et al., 2018), which leads to a enrichment of leaf water compared with source water (Cernusak et al., 2016; Dongmann et al., 1974). Given that oxygen isotopes share the same hydrological pathways as δ^2H_c, a strong connection between the two isotopes would be expected (Brooks et al., 2010; Dansgaard, 1964; Edwards and Fritz, 1986), as shown in wet regions where the two isotopes show strong positive correlations (An et al., 2014). However, biochemical processes appear to shape oxygen and hydrogen isotope ratios differently under distinct climatic conditions, and ^2H-fractionations before and during cellulose synthesis are more variable than ^{18}O-fractionations (Luo and Sternberg, 1992; Yakir and DeNiro, 1990). Photosynthetic isotope fractionation induces a relatively constant ^{18}O-enrichment of sugars compared with leaf water (Lehmann et al., 2021b). On the contrary, there is a not yet fully quantified ^2H-depletion in plant sugars compared with leaf water (Dunbar and Schmidt, 1984), which varies with environmental conditions and species (Lehmann et al., 2021a). In particular, for mature trees, post-photosynthetic isotope fractionations during the transport of sugars to sink tissues have been partly quantified for $\delta^{18}O_c$ (Gessler et al., 2014; Treydte et al., 2014), but are still not fully resolved for δ^2H_c. Recent literature suggests that the use of carbon reserves causes an additional ^2H-enrichment in leaf and tree-ring cellulose (Cormier et al., 2018; Kimak et al., 2015; Lehmann et al., 2021b). It remains uncertain to what extent δ^2H_c acts as a hydrological and climatic indicator, as observed for $\delta^{18}O_c$ (Treydte et al., 2007), and whether δ^2H_c stores information on plant metabolism, physiology, and carbon allocation (Cormier et al., 2018; Lehmann et al., 2021b; Sanchez-Bragado et al., 2019).

Mechanistic models are an important tool for interpreting of tree-ring isotope data. They have been developed and applied for the simulation of $\delta^{18}O_c$ records in relation to hydrological (Sargeant et al., 2019), climatological signals (Saurer et al., 2016), as well as for $\delta^{13}C_c$ simulations that provided physiological information (Guerrieri et al., 2019; Lavergne et al., 2020), while it

has been seldomly applied for the modelling of δ^2H_c in tree rings (Nabeshima et al., 2018; Nakatsuka et al., 2020a, 2020b; Voelker et al., 2014). Specifically, the model of Roden and Ehleringer (2000); hereafter RE-model, is currently the applied model used to estimate δ^2H_c in tree rings by taking into account the isotopic variation from hydrological sources (i.e. source water, water vapour, leaf water), as well as photosynthetic and post-photosynthetic isotope fractionations (autotrophic and heterotrophic), before and during stem cellulose biosynthesis (Roden and Ehleringer, 2000). Some of the RE-model parameters, which were previously considered as constants, have been found to have temporal variability, as for example in the isotope exchange rates between xylem and leaf water during cellulose formation (*f*), which exhibited variations among species and tissues (Cernusak et al., 2005; Song et al., 2014), and in the dependence on environmental conditions (Cheesman and Cernusak, 2017; Sternberg and Ellsworth, 2011). However, these studies focused on the variation of $\delta^{18}O_c$ and included only on few species mostly in controlled experiments, and therefore, the conclusions are not fully utilisable for the modelling of δ^2H_c in natural conditions. Furthermore, recent findings suggest that important processes causing hydrogen isotope fractionations in plants are not yet integrated into the RE-model, which may lead to miss-estimations as, for example the isotope fractionations of enzymatic reactions connected to (i) the use of carbohydrate reserves (Kimak and Leuenberger, 2015; Nakatsuka et al., 2020a), (ii) environmental inputs (i.e. light and CO_2), (iii) species-specific mechanisms (Arosio et al., 2020a; Cormier et al., 2018; Sanchez-Bragado et al., 2019). However, so far only few attempts have been made to address δ^2H_c variability at a continental scale, showing considerable within-site variability (Nakatsuka et al., 2020a; Voelker et al., 2014). The extent to which large-scale or inter-annual variations can be captured by the RE-model remains largely unknown, and the potential mis-estimations have yet to be quantified. Therefore, the interpretations of the RE-model results should be considered carefully in light of its limitations.

The European isotope network ISONET offers the opportunity to evaluate tree-ring cellulose isotope chronologies (i.e. $\delta^{13}C_c$, $\delta^{18}O_c$, δ^2H_c) and tree-ring-width chronologies (TRW) for two genera (*Pinus*, *Quercus*) over the past 100 years for 17 sites from Finland to Spain, and Poland. High common variance of $\delta^{13}C_c$ and $\delta^{18}O_c$ was shown by Treydte et al. (2007), and several site-specific analyses have been carried out during the past decade (see publication list Table S.1). The present study focuses on assessing spatiotemporal δ^2H_c patterns across Europe for the first time, leveraging the unique and extensive ISONET δ^2H_c network. Here, we systematically assessed the performance of δ^2H_c as a potential climatic and physiological indicator for the different functional genera. Specifically, we investigated (i) the low- and high-frequency variability of the δ^2H_c time series; (ii) the long- and short-term climate signals captured by δ^2H_c; (iii) how δ^2H_c relates to $\delta^{18}O_c$ and TRW; and finally (iv) the ability of mechanistic models to predict δ^2H_c values at a continental scale. Accordingly, we hypothesized that:

1. The climatic information recorded in δ^2H_c high-frequency chronologies:
   a. shows lower strength and lower large-scale agreement compared with the $\delta^{13}C_c$ and $\delta^{18}O_c$ chronologies.
   b. is specific to each genus, due to different physiological mechanisms.
   c. shows genus-specific responses for extreme climatic conditions.
2. The δ^2H_c relationships with TRW are stronger than those with $\delta^{18}O_c$, indicating a larger share of physiological information than hydrological signals.
3. The RE-model successfully estimates the continental-scale climatic effect on δ^2H_c, but not the year-to-year variation.

2. Methods

2.1. Tree-ring chronologies and isotope analyses

2.1.1. European tree-ring network and climate data

ISONET is a European tree-ring isotope network that includes Mediterranean, humid-temperate, continental, and subarctic climatic regions. The sites are distributed along a latitudinal (37°81′ to 68°93′ N), longitudinal (−5°25′ to 30°93′ E), and elevational gradient (5 to 2′100 m a.s.l.), with high-elevation sites concentrated at lower latitudes. The selected sites are old-growth forests (mean ± SD of age = 454 ± 196 years) with two main genera (*Quercus* and *Pinus*, Table 1). Spatiotemporal patterns of the TRW, $\delta^{18}O_c$, and $\delta^{13}C_c$ chronologies have been explored across the entire network (Balting et al., 2021; Shestakova et al., 2019; Treydte et al., 2007) and with 18 site-level studies (see citation list in Table S.1). However, although the δ^2H_c chronologies were measured and analysed with an annual resolution (1905–2002) at 17 sites of the ISONET network (Table 1), results from only 5 sites have been published individually so far (Etien et al., 2009; Haupt et al., 2011; Hilasvuori and Berninger, 2010; Loader et al., 2008; Szczepanek et al., 2006).

For each study site, monthly climate data were extracted from the Climatic Research Unit, CRU TS4.03 for the period 1905–2002 (Harris et al., 2020), including mean temperature, precipitation and atmospheric water vapour. Monthly vapour pressure deficit (VPD) was calculated as the difference between measured water vapour and the temperature-dependent saturated humidity value (e_{sat}):

$$e_{sat} = 6.1078^{\left(a\frac{T-273.16}{T-b}\right)}$$

where T is the average monthly temperature and where a = 21.87 and b = 7.66 at $T > 0$ and a = 17.27 and b = 35.86 at $T > 0$, as described by Murray (1967). Across all sites for the June–July–August period, the mean temperature (MT_{JJA}) ranged from 11 °C to 23 °C, total precipitation (MP_{JJA}) from 35 mm to 590 mm, and VPD (VPD_{JJA}) from 2.4 to 14.2 (hPa).

2.1.2. Study species

The network contains data from two functionally different genera: *Pinus* (*Pinus sylvestris* L., *Pinus uncinata* Ram. and *Pinus nigra* Arn.) and *Quercus* (*Quercus petraea* (Matt.) Liebl. and *Quercus robur* L.) (Table 1). *Pinus* sites are mostly located in boreal and high-elevation Mediterranean zones, while *Quercus* sites dominate western and central European lower elevations.

Pinus and *Quercus* species are widely distributed over Europe and are both ecologically and economically important. They have contrasting ecophysiological characteristics (Bréda et al., 2006; Bréda and Badeau, 2008; Merlin et al., 2015; Michelot et al., 2012a) and use opposite strategies to cope with periods of severe drought (Hochberg et al., 2018; Tyree and Cochard, 1996; Zweifel et al., 2009). *Pinus* is an evergreen coniferous genus with isohydric characteristics, which implies high stomatal control through a tight and continuous water potential homeostasis (Irvine et al., 1998; Leo et al., 2014; Salmon et al., 2015) and generally a shallow root system (Grossiord et al., 2014; Laitakari, 1927). In contrast, the deciduous broadleaf *Quercus* genus, exhibits an anisohydric behaviours keeping stomata open and high photosynthetic rates for long time periods (Aranda et al., 2000; Bréda et al., 1993; Klein, 2014), and typically has a deep root system with a large taproot and strong lateral roots (Zapater et al., 2011).

2.1.3. Tree-ring width and stable isotope measurements

Increment cores were extracted at breast height from dominant old-growth trees at all sites (on average 46 trees per site). Following standard dendrochronological procedures (Cook and Kairiukstis, 1990), tree rings were visually crossdated and tree-ring widths (TRW) were measured at 0.01 mm precision. Cross-dating validation was carried out following standard procedures (Holmes, 1983). From at least four trees per site, dated tree rings were cut and annually pooled, and cellulose was extracted using standard extraction and purification methods (Boettger et al., 2007). Whole tree rings were pooled for the isotope analysis of *Pinus*. For *Quercus* only the latewood was used, as the δ^2H-values of early- and latewood in *Quercus* species have been shown to have a clear offset, although strongly correlated (r^2 = 0.63), (Kimak, 2015), and in order to avoid undesired signals from previous-year carbohydrate reserves (Helle and Schleser, 2004). For the Swiss Cavergno site (CAV) no separation between early- and latewood was possible because the rings were too narrow.

Table 1
Site details on species composition, geography, and climate ordered by latitude (North to South). Climatic variables represent the means of the common study period (1905–2002), obtained from CRU TS4.03. MT_{JJA} = mean air temperature, MP_{JJA} = mean precipitation, and VPD_{JJA} = mean vapour pressure deficit, all for the months of June, July, and August; TRW = mean tree-ring width; isotope ratios of tree-ring cellulose ($\delta^{13}C_c$, $\delta^{18}O_c$, δ^2H_c); δ^2H_{sw} = modelled hydrogen source water.

Site code	Site name	Country	Species	Lat (°N)	Lon (°E)	Elev. (m a.s.l.)	MT_{JJA} (°C)	MP_{JJA} (mm)	VPD_{JJA} (hPa)	TRW (mm)	$\delta^{13}C_c$ (‰)	$\delta^{18}O_c$ (‰)	δ^2H_c (‰)	δ^2H_{sw} (‰)
INA	Kessi/Inari	Finland	*P. sylvestris*	68.93	28.42	150	11.7	169	3.9	0.52	−24.4	26.4	−95.6	−106
ILO	Ilomantsi	Finland	*P. sylvestris*	62.98	30.98	200	14.8	192	4.6	0.29	−23.7	27.1	−106.1	−91.1
GUT	Gutulia	Norway	*P. sylvestris*	62.00	12.18	800	11.4	234	3.5	0.49	−23.3	27.6	−94.3	−99.6
BRO	Bromarv	Finland	*Q. robur*	60.00	23.08	5	15.3	189	4.1	1.85	−24.8	25.6	−93.3	−82.0
LCH	Lochwood	Scotland	*Q. robur*	55.27	−3.43	175	12.9	325	2.4	1.16	−25.2	27.9	−46.3	−60.9
PAN	Panemunes Silas	Lithuania	*P. sylvestris*	54.88	23.97	45	16.7	226	4.9	0.79	−22.9	28.7	−67.9	−67.6
SUW	Suwalki	Poland	*P. sylvestris*	54.10	22.93	160	16.7	235	4.6	1.02	−23.1	28.5	−76.1	−73.4
WOB	Woburn	UK	*Q. robur*	51.98	−0.59	50	15.7	169	3.9	1.37	−23.3	29.1	−54.1	−52.8
DRA	Dransfeld	Germany	*Q. petraea*	51.5	9.78	320	15.8	227	7.5	1.41	−23.5	28.7	−19.6	−56.3
WIN	Windsor	UK	*P. sylvestris*	51.41	−0.59	10	15.7	155	3.8	0.47	−22.9	30.4	−31.7	−48.5
GIB	Niopolomice Gibiel	Poland	*Q. robur*	50.12	20.38	190	17.2	277	4.8	1.87	−25.7	27.8	−76.6	−62.6
POE	Poellau	Austria	*P. nigra*	47.95	16.06	500	17.5	289	5.3	0.62	−24.2	27	−59.8	−65.5
VIG	Vigera	Switzerland	*P. sylvestris*	46.5	8.77	1400	12.2	589	3.2	0.47	−23.1	30.8	−45.7	−110.0
CAV	Cavergno	Switzerland	*Q. petraea*	46.35	8.60	900	12.2	589	3.2	1.11	−23.3	29.2	−51.2	−86.6
LIL	Pinar de Lillo	Spain	*P. sylvestris*	43.07	−5.25	1600	16.3	143	5.6	0.47	−22.2	30.9	−46.1	−65.2
PED	Pedraforca	Spain	*P. uncinata*	42.24	1.70	2100	16.1	214	6.1	0.49	−21.9	30.8	−32.1	−45.1
CAZ	Cazorla	Spain	*P. nigra*	37.81	−2.96	1816	23.2	36.3	14.2	0.471	−21.1	33.6	−26.4	−48.7

The extracted cellulose was then split in three parts for the analysis of the three isotope ratios. The details of $\delta^{18}O_c$ and $\delta^{13}C_c$ analyses are described in Treydte et al. (2007) and in the site-specific publications listed in Table S.1. For the δ^2H_c analysis the cellulose was subjected to two different procedures: nitration and equilibration. In the first case, a complete removal of all exchangeable OH-groups was achieved by nitration (Boettger et al., 2007; Green, 1963), while in the second case, the exchangeable H was set at a known isotope value through the equilibration with water vapour, which enabled the δ^2H-values of the non-exchangeable H to be calculated by mathematical correction (Schimmelmann, 1991; Wassenaar and Hobson, 2003). Both procedures produce comparable results as shown by Filot et al. (2006). The proceedings conducted at each lab and the details are given in Table S.2. For both methods, samples were subsequently converted to H_2 by high-temperature pyrolysis and analysed by IRMS with a precision of ca. ±2‰. The δ^2H_c values of all sites are referenced to the Vienna Standard Mean Ocean Water (VSMOW).

The low-frequency domain of the 17 δ^2H_c chronologies was explored for the common period 1905–2002 by applying a 100-year smoothing spline (Cook and Kairiukstis, 1990), whereas the high-frequency domain (year-to-year variation) was obtained by calculating the first-order differences (FDiff) for TRW, $\delta^{13}C_c$, $\delta^{18}O_c$, and δ^2H_c a stationary mean was obtained to avoid autocorrelation, and to highlight interannual variability. The agreement among sites in the low and high frequency domains of the δ^2H_c chronologies was assessed with pairwise correlations using the 'corr' function in the *base* package in R. All computations were performed using the R version 4.0.3 (R Core Team, 2020), and graphics were produced using the R package *ggplot2* (Wickham, 2016).

2.2. Climate sensitivity analyses

For comparisons with the FDiff chronologies, the same detrending was applied to the climate data: monthly temperature (T), precipitation (P), and vapour pressure deficit (VPD) series. Bootstrapped Pearson's correlations were performed between FDiff chronologies and FDiff climate series for the common period 1905–2002 using the R package *treeclim* (Zang and Biondi, 2015). All correlations were calculated for single months and for 3-month windows of the current year (April–May–June, June–July–August, August–September–October). Because, the June–July-August period yielded the highest correlations for all variables (Fig. S.1), it was the selected period for further climate analyses. Pearson's correlation coefficients between the high-frequency variation (FDiff) of TRW and isotope chronologies with climate variables are indicated as $X_{\text{-signal}}$ (e.g. $\delta^2H_{\text{c-signal}}$).

First, the spatial patterns of the obtained climate correlations across the entire network were assessed. To evaluate the differences in $TRW_{\text{-signal}}$, $\delta^{13}C_{\text{c-signal}}$, $\delta^{18}O_{\text{c-signal}}$, and $\delta^2H_{\text{c-signal}}$ for each species and climate variable, analyses of variance (ANOVA), Tukey's post hoc tests, and Bonferroni corrections were performed on absolute values of the climate correlations. Significance level was set at $P < 0.05$.

The sensitivity of FDiff δ^2H_c chronologies to extreme climatic conditions was also assessed. Years with positive (wet) and negative (dry) extreme values in summer P-PET (precipitation minus potential evapotranspiration) were selected at the site level by setting a threshold of +1.5 (wet) or −1.5 (dry) standard deviation from the average value. Summer potential evapotranspiration (PET) was calculated with the Thornthwaite method (Thornthwaite, 1948) using the R package *SPEI* (Vicente-Serrano et al., 2010). Significant differences between genera, extreme events, and their interactions were evaluated through analyses of variance (two-way ANOVA), Tukey's post hoc tests, and Bonferroni corrections.

For an assessment of the potential physiological and hydrological information in δ^2H_c, the relationships between the δ^2H_c and TRW chronologies, and between the δ^2H_c and $\delta^{18}O_c$ chronologies (both measured and FDiff) were investigated at site level using linear models. Further, the slopes from these relationships were assessed against mean precipitation (MP_{JJA}) and mean temperature (MT_{JJA}) in June–July–August (Table 1) and fitted with a polynomial function and a quadratic fit.

2.3. Mechanistic modelling of tree-ring δ^2H_c

Physiological mechanisms linked to the geographical patterns and temporal variability of our isotope chronologies were investigated by mechanistically modelling δ^2H values for leaf water and tree-ring cellulose. Leaf water δ^2H values (δ^2H_{lw}) were estimated using the Craig Gordon Model (CG-Model) at the evaporative site (Craig and Gordon, 1965; Dongmann et al., 1974):

$$\delta^2H_{lw} = \delta^2H_{sw} + \varepsilon_k + \varepsilon_e + \left(\delta^2H_v - \delta^2H_{sw} - \varepsilon_k\right) * {}^{e_a}/_{e_i} \quad (1)$$

where e_a/e_i reflects the water vapour partial pressures outside and inside the leaf, ε_e and ε_k are temperature-dependent equilibrium and kinetic fractionation factors (Table 2), respectively, δ^2H_{sw} is the hydrogen isotope ratio

of the source water, and δ^2H_v is the atmospheric water vapour. Assuming equilibrium between δ^2H_{sw} and δ^2H_v, and that e_a/e_i is the mean annual relative humidity (*RH*) (Cernusak et al., 2016), Eq. (1) was transformed to:

$$\delta^2H_{lw} = \delta^2H_{sw} + (\varepsilon_k + \varepsilon_e + (-\varepsilon_e - \varepsilon_k)) * RH \quad (2)$$

δ^2H_{lw} was calculated annually for each site using mean summer temperatures and constant δ^2H_{sw} estimates for each site (Table 1), extrapolated from the gridded data as defined by Bowen (2008). A generalized model was used and no further corrections for unenriched leaf water pools (Péclet effect) were applied (Roden et al., 2015) due to the lack of species-specific correction factors (Arosio et al., 2020b; Voelker et al., 2014). These dilution effects have been shown to be difficult to estimate accurately and to have large differences between subspecies and over time (Song et al., 2014). They require extensive physiological measurements that are not available for these species and timescales and have therefore not been included in the model to avoid unquantifiable errors.

The CG-Model can be extended to organic material, such as tree rings, using the RE-model (Roden and Ehleringer, 2000).

$$\delta^2H_cRE\ (‰) = f * \left(\delta^2H_{sw} + \varepsilon_h\right) + (1 - f) * \left(\delta^2H_{lw} + \varepsilon_a\right) \quad (3)$$

where ε_a and ε_h are the specific autotrophic and heterotrophic ^{2}H-biosynthetic fractionation factors, respectively, and f is the specific fraction before tree-ring cellulose synthesis (Table 2).

3. Results

3.1. High- and low-frequency variability in the δ^2H_c site chronologies

The δ^2H_c chronologies showed a 75‰ difference in absolute values between the northern-most sites (INA, ILO, and GUT) with the lowest values and the Spanish site (CAZ) with the highest values (Fig. 1a, b). Over the course of the 20th century there was no clear common trend among the site δ^2H_c mean values, except for the last 10 years when a positive trend occurred at most *Quercus* sites (Fig. 1b) and for a few *Pinus* sites especially at higher latitudes (Fig. 1a). The long-term trends showed strong site-to-site variability and sparse significant correlations ($P < 0.05$) between sites (Fig. S.2a), with clusters consisting of the three Spanish sites, the Polish and British sites, and the two Swiss sites.

The year-to-year variability retained in the site FDiff δ^2H_c chronologies were of a similar range within and between sites (Fig. 1c, d), with smaller variance for *Quercus* than *Pinus*. The FDiff δ^2H_c chronologies of some geographically close sites were significantly correlated ($r = 0.4$, CAV–VIG, ILO–GUT; $r = 0.3$, PAN–SUW, LIL–PED–CAZ), while this agreement was reduced among sites that were farther apart (Fig. S.2b).

3.2. Climate correlations

3.2.1. Spatial patterns and species-specific differences

In general, $\delta^2H_{c\text{-signal}}$ was negative regarding summer precipitation and positive regarding summer temperature and VPD across the whole network (Fig. 2a). No clear latitudinal pattern was observed for the $\delta^2H_{c\text{-signal}}$ and any climatic parameter. However, at the fringes of the network, the strength in the $\delta^2H_{c\text{-signal}}$ of the northernmost sites was lower than at the southernmost ones, especially for *Pinus*. The $TRW_{\text{-signal}}$ was highly site-specific (Figs. 3, S.3), with no clear latitudinal gradient. At sites with a high $TRW_{\text{-signal}}$, we observed a low $\delta^2H_{c\text{-signal}}$ ($r \sim 0$, INA), and vice versa ($r \sim 0.5$, CAV), although this negative relationship between $TRW_{\text{-signal}}$ and $\delta^2H_{c\text{-signal}}$ was not consistent across the network.

The $\delta^{13}C_{c\text{-signal}}$ and $\delta^{18}O_{c\text{-signal}}$ were generally high (up to $r = 0.7$) and were negative regarding summer precipitation and positive regarding temperature and VPD (Figs. 3, S.3). Contrary to the $\delta^2H_{c\text{-signal}}$, temperature and VPD-$\delta^{13}C_{c\text{-signal}}$ showed a distinct latitudinal gradient, with strong correlations at higher latitudes and the British sites. In comparison, no distinct latitudinal trend was observed for the $\delta^{18}O_{c\text{-signal}}$, although the northern sites generally showed lower correlations with summer temperature and VPD than the southern sites.

We detected significant differences in climate sensitivity between genera, as the summer temperature $\delta^2H_{c\text{-signal}}$ in *Pinus* was significantly higher than in *Quercus*, resulting in significant differences between their climate signals (Table S.3). Specifically, for *Pinus*, the absolute $\delta^2H_{c\text{-signal}}$ was consistent for all climatic parameters ($r \sim 0.3$), but it was significantly lower than the absolute $\delta^{13}C_{c\text{-signal}}$ for all climate parameters, and significantly lower than $\delta^{18}O_{c\text{-signal}}$ for precipitation and VPD (Fig. 3). For *Quercus*, the absolute $\delta^2H_{c\text{-signal}}$ was significantly lower than the absolute $\delta^{18}O_{c\text{-signal}}$ and $\delta^{13}C_{c\text{-signal}}$ for all climate parameters (Fig. 3). Interestingly, no significant differences were found between $\delta^2H_{c\text{-signal}}$ and $TRW_{\text{-signal}}$ of the two genera for any climatic variable (Fig. 3). Regarding changes along the gradients of precipitation and temperature covered by the sites, no significant effect was found in the climate signal strength recorded by *Pinus* δ^2H_c (Fig. 4). Conversely, for *Quercus* the strength of the temperature-$\delta^2H_{c\text{-signal}}$ increased significantly along the precipitation gradient and decreased along the temperature gradient (Fig. 4c, d), while the strength of the precipitation-$\delta^2H_{c\text{-signal}}$ did not vary significantly along the gradients, indicating a stronger impact of temperature on the δ^2H-variations particularly at cool and wet sites.

3.2.2. Comparison of the climate signals recorded in δ^2H_c and $\delta^{18}O_c$

When examining the relationship between $\delta^2H_{c\text{-signal}}$ and $\delta^{18}O_{c\text{-signal}}$ ($H\text{-}O_{\text{-signal}}$) across the whole network, we observed a divergence between the two genera with decreasing latitude (Fig. 5). *Pinus* showed a negative $H\text{-}O_{\text{-signal}}$ for all three climate variables (significant for precipitation and VPD, but not for temperature). On the contrary, *Quercus* showed a positive

Table 2
Summary of fractionation factors for the modelling of δ^2H_c and corresponding literature sources.

CG-model			
Kinetic fractionation factor			
ε_k	H	25‰	(Cernusak et al., 2016; Merlivat, 1978)
Equilibrium fractionation factor			
ε_e	H	$e_e = \exp\left(\left(\frac{24.844}{(273.16+T_{mean})^2}\right) * 1000\right) - \left(\left(\left(\frac{76.248}{273.16+T_{mean}}\right) + 0.052612\right) - 1\right) * 1000$	Temperature dependent (Cernusak et al., 2016; Majoube, 1971)
RE-model			
Fraction of exchange before cellulose synthesis			
f	H	0.36	(Roden and Ehleringer, 1999)
Biosynthetic fractionation factors			
ε_a	H	−171‰	Autotrophic fractionation (Yakir and DeNiro, 1990)
ε_h	H	158‰	Heterotrophic fractionation (Yakir and DeNiro, 1990)

Fig. 1. The δ^2H_c site chronologies for Pinus (a) and Quercus (b) for the common period (1905–2002), and their low-frequency variability illustrated by a 100-year smoothing spline (dashed lines). The corresponding high-frequency site chronologies calculated as first differences (FDiff) are given for *Pinus* (c) and *Quercus* (d). Site colours are ordered by latitude (North to South in the legend). (For interpretation of the references to colour in this figure legend, the reader is referred to the web version of this article.)

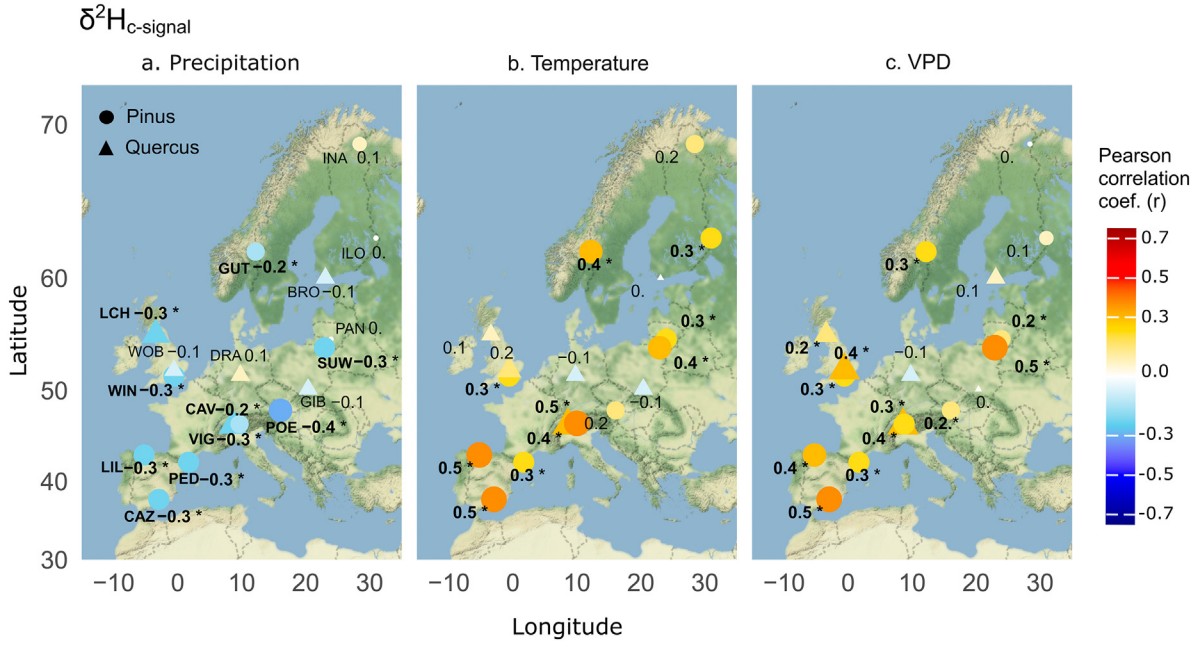

Fig. 2. Mapping of Pearson's correlation coefficients of the FDiff δ^2H ($\delta^2H_{c\text{-signal}}$) with summer (June–July–August) climate variables (precipitation, temperature, and vapour pressure deficit (VPD), also as FDiff). Significant correlations ($P < 0.05$) are indicated by asterisks.

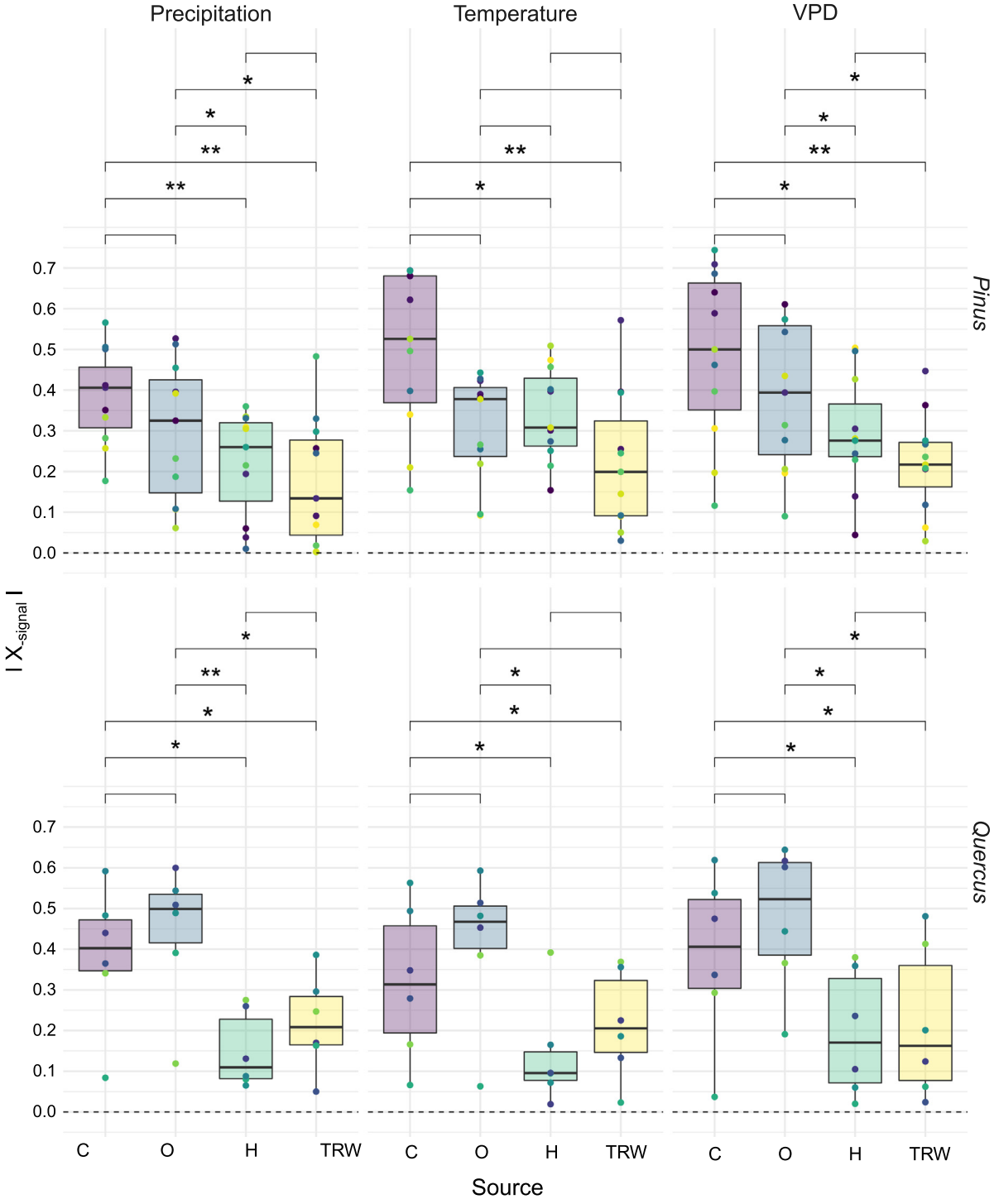

Fig. 3. Differences in the absolute $\delta^{13}C_{c\text{-signal}}$ (C), $\delta^{18}O_{c\text{-signal}}$ (O), $\delta^{2}H_{c\text{-signal}}$ (H), and $TRW_{\text{-signal}}$ (TRW) for summer (June–July–August) climate variables (precipitation, temperature, and VPD) for the genera *Pinus* (top panel) and *Quercus* (bottom panel) (Table S.3). Significant differences between pairs are indicated by asterisks ($P < 0.05$ = *, $P < 0.01$ = **). The colour of the points indicates the sites, as shown in Fig. 1. (For interpretation of the references to colour in this figure legend, the reader is referred to the web version of this article.)

H-$O_{\text{-signal}}$ for temperature and VPD, and a negative one for precipitation (although none of these trends were significant).

At northern sites the two genera showed similar values for $\delta^{18}O_{c\text{-signal}}$ and $\delta^{2}H_{c\text{-signal}}$ regarding temperature and VPD ($\delta^{18}O_{c\text{-signal}}$ $r = 0.5$; $\delta^{2}H_{c\text{-signal}}$ $r = 0.2$). On the contrary, at southern sites where $\delta^{18}O_{c\text{-signal}}$ was around 0 for both genera, $\delta^{2}H_{c\text{-signal}}$ increased for *Pinus* (r = 0.5) and decreased for *Quercus* ($r = 0.1$). For example, in Finland (*Pinus*) the VPD $\delta^{18}O_{c\text{-signal}}$ was 0.6 and the VPD $\delta^{2}H_{c\text{-signal}}$ was 0.01. On the contrary, in Spain (*Pinus*) the VPD $\delta^{18}O_{c\text{-signal}}$ was −0.2 and the VPD $\delta^{2}H_{c\text{-signal}}$ was 0.5. Similarly, in the UK (*Quercus*), where $\delta^{18}O_{c\text{-signal}}$ showed strong correlations with VPD, $\delta^{2}H_{c\text{-signal}}$ showed only weak correlations.

3.2.3. Responses of $\delta^{2}H_{c}$ to summer climate extremes

We investigated the influence of particularly dry and wet summers on $\delta^{2}H_{c}$ by correlations to P-PET. Climatic conditions had a significant

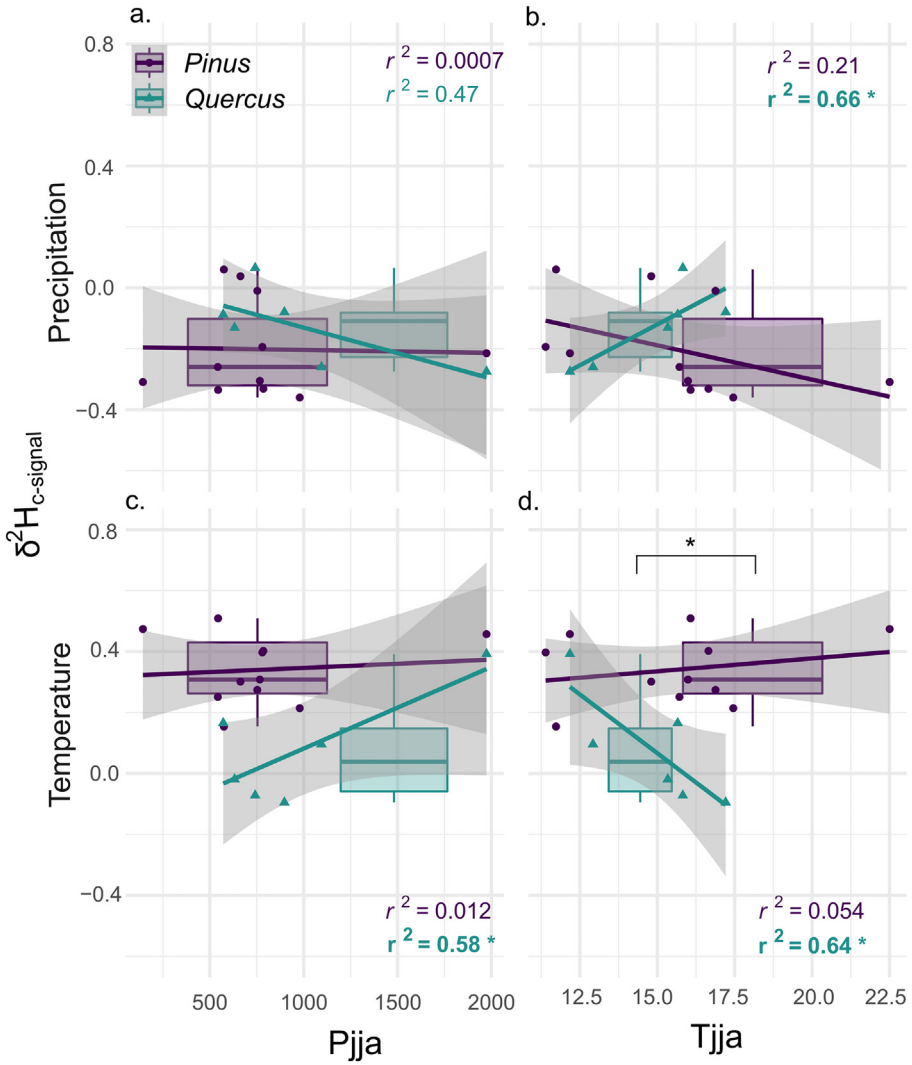

Fig. 4. Relationships between average summer precipitation (Pjja) and the $\delta^2H_{c\text{-signal}}$ (Pearson's correlation coefficients) for precipitation (a) and temperature (c), and between average summer temperature (Tjja) and the $\delta^2H_{c\text{-signal}}$ for precipitation (b) and temperature (d). *Pinus* and *Quercus* are shown separately. Points reflect single site's $\delta^2H_{c\text{-signal}}$ values. Significant differences between pairs are indicated by asterisks ($P < 0.05$ = *, $P < 0.01$ = **). The size of the boxes is dependent on the genera's ranges on the x axis.

effect on the FDiff δ^2H_c for both genera, while the δ^2H_c differences between the two genera were not significant (Table S.4). On average, dry summers (−1.5 SD from the mean P-PET for the June–July–August period) had significantly higher values of δ^2H_c, by 3‰ for both genera, compared with years with normal summer conditions (Fig. 6). The δ^2H_c values in years with wet summers (+1 SD) were not significantly different from the values in normal years for either genus. *Pinus* showed continuously increasing δ^2H_c from wet to dry years (Fig. 6a), whereas the δ^2H_c values of *Quercus* were not significantly different in wet years than in dry and normal years (Fig. 6b).

3.3. Relationships between δ^2H_c and $\delta^{18}O_c$ and between δ^2H_c and TRW

We found a significant positive relationship between the δ^2H_c and $\delta^{18}O_c$ for 10 of the 17 sites (Fig. 7a), while only 2 sites showed a significant negative relationship (Table S.5). The explained variance (r^2) ranged from 0.003 to 0.2, and the slopes from −4.2 to 3.6 (Table S.5). Regarding the relationship between the FDiff δ^2H_c and FDiff $\delta^{18}O_c$, 11 of the 17 sites showed a significant positive correlation, whereas only one site showed a significant negative correlation, with the slopes ranging from −1.8 to 4.1, and the r^2 from 0.01 to 0.28 (Fig. S.5, Table S.5). When analysing the effect of mean climate conditions on the FDiff δ^2H_c and FDiff $\delta^{18}O$ relationships, we observed a non-linear relationship along the MT_{JJA} gradient, with the highest slopes at 5 °C (r^2 = 0.4). On the contrary, a linear relationship between δ^2H_c-$\delta^{18}O_c$ slopes and MP_{JJA} was found (r^2 = 0.5) (Fig. S.8).

The linear relationships between the δ^2H_c and TRW records were highly variable and site-specific, with both positive (4 of 7 sites significant) and negative slopes (7 of 10 sites significant) (Fig. 7b), r^2 ranged from 0.002 to 0.33, and slopes ranged from −22 to 32 (Table S.5). For the FDiff standardized data the linear site-level models showed lower r^2 values (0.001 to 0.32), and only 9 of the 17 sites showed a significant relationship (3 positive and 4 negatives; Fig. S.5, Table S.5). The slopes of the FDiff δ^2H_c and TRW relationships had lower r^2 values (0.2) than those of the δ^2H_c and $\delta^{18}O$ relationships, and in both cases the slopes decreased with increasing temperature and precipitation (Fig. S.5, Table S.5).

3.4. Mechanistic modelling of the tree-ring isotope ratios

The RE-model captured the continental-scale mean δ^2H_c levels but did not capture the year-to-year site variability. The alignment of the fitted linear models between observed and predicted δ^2H_c values across several sites in Europe (Fig. 8 black dotted line) showed r^2 values of 0.46 and 0.33 and slopes of 0.76 and 0.91 for *Pinus* and *Quercus*, respectively. However, we observed a consistent overestimation of the modelled compared with the

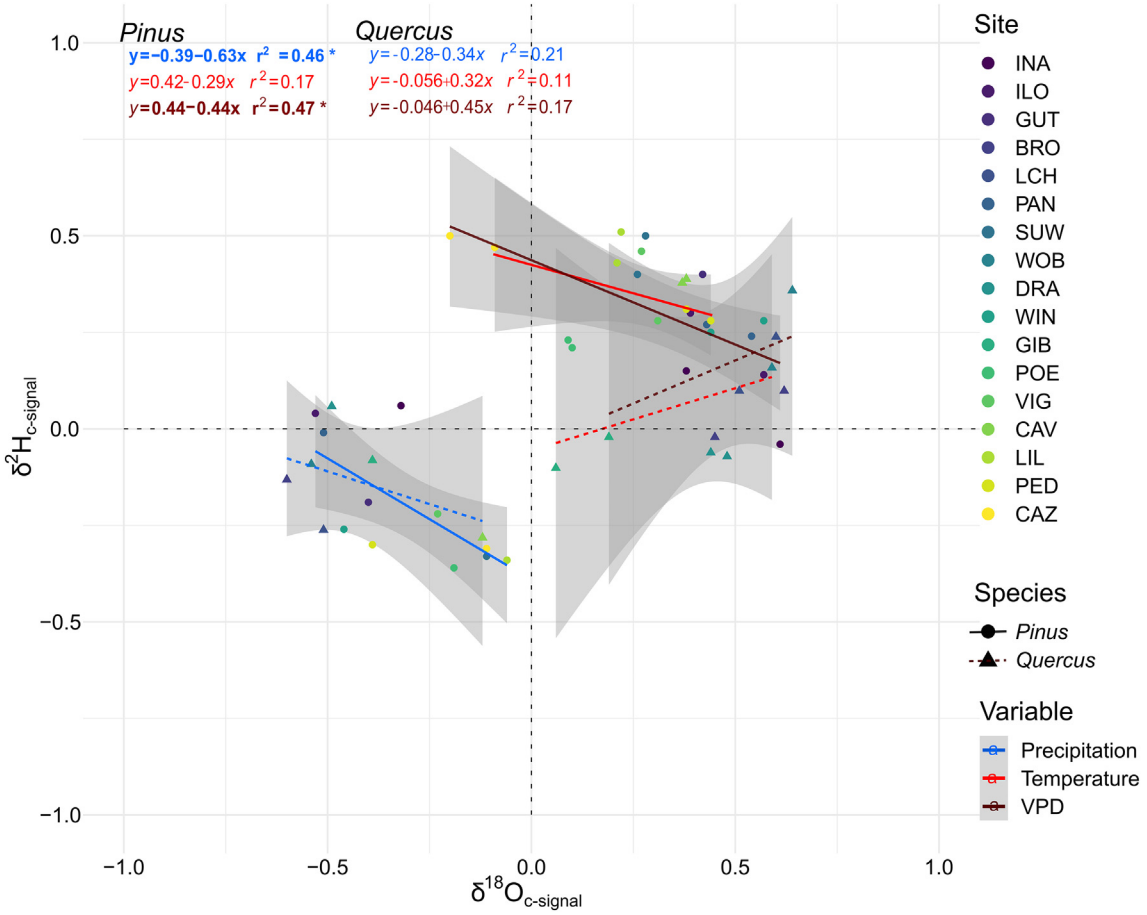

Fig. 5. Linear relationships between $\delta^2H_{c\text{-signal}}$ and $\delta^{18}O_{c\text{-signal}}$ (H-$O_{\text{-signal}}$) regarding precipitation, temperature, and VPD per genus (*Pinus* and *Quercus*). Site colours are ordered by latitude (North to South). Linear models are fitted for each climatic variable and genus, and significant relationships ($P < 0.05$) are indicated by asterisks. Pinus regressions are indicated by solid lines and Quercus regressions by dashed lines. (For interpretation of the references to colour in this figure legend, the reader is referred to the web version of this article.)

measured δ^2H_c values by an average of 43‰ for both species (Fig. 8, Table S.6). For *Quercus*, the fitted linear model had a slope of 0.91, indicating an almost constant model performance across all sites. For *Pinus*, the fitted linear model had a slope of 0.7, indicating better model performance for high-latitude sites. The Swiss sites VIG (*Pinus*) and CAV (*Quercus*) showed the largest offset between measured and modelled values, i.e. 99.5‰ and 70.7‰, respectively. These two study sites have the same climate data, being in the same interpolation cell, although they differ in elevation by 500 m. For this reason, a second linear model excluding these two sites was calculated, resulting in an improvement of the general model fit for both genera ($r^2 = 0.83$ and 0.69, slope = 1.2 and 1.7 for *Pinus* and *Quercus*, respectively), resulting in an improved fir for higher latitudes sites (Fig. 8). Independently of the dataset used, the year-to-year variability within the sites was not captured by the model (the average values of the FDiff model are $r^2 = 0.04$ and 0.02, slope = 0.6 and 0.4 for *Pinus* and *Quercus*, respectively; Fig. S.7).

4. Discussion

4.1. Low- and high-frequency variations in the δ^2H_c chronologies

This is the first European-scale study exploring 100-year δ^2H_c chronologies in both low- and high-frequency domains (Fig. 1). The ^{2}H-depletion with increasing latitude follows the naturally occurring isotopic variations in precipitation (i.e. Global Meteoric Water Line, Fig. S.9; (Allen et al., 2019; Craig, 1961; Craig and Gordon, 1965)), independent of the two genera. The comparison of the long-term trends among sites resulted in relatively low, sporadic significant correlations (Fig. S.3a). In the last decade, a relative ^{2}H-enrichment was apparent at most of the sites, particularly those with *Quercus* (Fig. S.1), although the strength of this increase was site-specific. The between-site agreement decreased when year-to-year variability was assessed. In this case, only relatively geographically close sites remained correlated (Fig. S.3b). The fact that these low- and high-frequency δ^2H_c patterns are very site specific, pose issues for further extrapolations of the $\delta^2H_{c\text{-signal}}$ (e.g. for climate reconstructions: Christiansen and Ljungqvist, 2017). Therefore, both frequency domains should be considered in future studies exploring the potential of δ^2H_c for dendroclimatological purposes.

4.2. The climate sensitivity of δ^2H_c across Europe compared with TRW, $\delta^{13}C_c$ and $\delta^{18}O_c$

In temperate forests, the strength of $\delta^{18}O_{c\text{-signal}}$ and $\delta^{13}C_{c\text{-signal}}$ across different climates has already been clearly shown in European networks (Shestakova and Martínez-Sancho, 2021; Treydte et al., 2007; Vitali et al., 2021), although biases connected to long-term trends have been reported (Esper et al., 2010) and a complete understanding of the related fractionation processes is still missing (Gessler et al., 2014). Nonetheless, these signals were clearly more consistent than the $\delta^2H_{c\text{-signal}}$. Our results confirm our first hypothesis (**Hp1a**), showing that the $\delta^2H_{c\text{-signal}}$ was on average weaker than the $\delta^{13}C_{c\text{-signal}}$ and $\delta^{18}O_{c\text{-signal}}$, but similar to the $TRW_{\text{-signal}}$ (Figs. 1, 2, S.2), with large variation at the continental scale. At the centre of our network, we observed the lowest temperature-$\delta^2H_{c\text{-signal}}$. However, significant correlations with

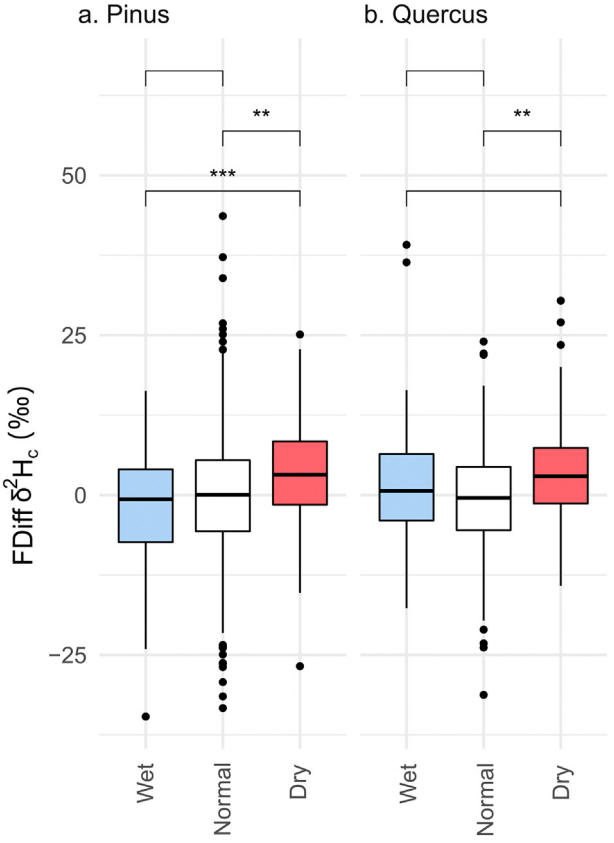

Fig. 6. The FDiff δ^2H_c differences among years with climatic characteristics different than the site P-PET mean (+1.5 SD = wet summer conditions and −1.5 SD = dry summer conditions; Fig. S.5) for the two studied genera (Table S.4). Significant differences between groups are indicated by asterisks ($P < 0.01$ = **; $P < 0.001$ = ***).

summer temperature (Szczepanek et al., 2006) and summer relative air humidity (Haupt et al., 2011) have been reported in some studies in Poland and Austria respectively.

The interplay of biological processes, at stand level (e.g. competition for light and nutrients: Giuggiola et al., 2016) and at tree physiological level (e.g. leaf gas exchange: Guerrieri et al., 2019, pollution: Boettger et al., 2014; Savard, 2010), can potentially mask the recorded $\delta^2H_{c\text{-signal}}$. The loss of climatic information in the δ^2H_c records could be due to (i) biochemical ^{2}H-fractionations at the leaf level (Yakir and DeNiro, 1990), (ii) kinetic isotope effects in biochemical reactions involved in the fixation of hydrogen in different positions of the glucose molecule (Augusti et al., 2006; Waterhouse et al., 2002), (iii) isotope fractionations and H-exchange with water during the biosynthesis of carbohydrates (Cormier et al., 2018). Thus, the $\delta^2H_{c\text{-signal}}$ can be assumed to be the result of the complex interaction between climatic and physiological processes, explaining why it is difficult to find one major climate driver at the continental scale or across climatic areas (Shestakova et al., 2019).

4.3. Genus-dependent differences in the climate sensitivity of δ^2H_c

We observed a significant genus dependency of the climate sensitivity of δ^2H_c (Figs. 3, 4), supporting our hypothesis (**Hp1b**). When comparing the functionally distant genera *Pinus* and *Quercus*, differences in the $\delta^2H_{c\text{-signal}}$ were evident, similar to $\delta^{13}C_{c\text{-signal}}$ and $\delta^{18}O_{c\text{-signal}}$ (Martínez-Sancho et al., 2018). *Pinus*' δ^2H_c climate sensitivity was stronger than that of *Quercus* for all climatic variables across the whole network (Fig. 3). A decoupling of H-$O_{\text{-signal}}$ between the two genera was observed at sites with a low temperature- and VPD-$\delta^{18}O_{c\text{-signal}}$, where *Pinus* showed a strong $\delta^2H_{c\text{-signal}}$, while *Quercus* showed a weak $\delta^2H_{c\text{-signal}}$ (Fig. 5). These contrasting signals are likely the result of different physiological mechanisms affecting isotope fractionation and water uptake dynamics, as explored below.

4.3.1. Use of fresh and stored photosynthates for cellulose formation

Hydrogen isotope patterns of leaf (Kimak et al., 2015) and tree-ring cellulose (Epstein and Yapp, 1976; Mayr et al., 2003) suggest that stored photosynthates in heterotrophic tissues (branches, stem, roots) are likely more ^{2}H-enriched than fresh photosynthates and that considerable use of carbohydrate reserves for growth could, lead to the observed bias in the $\delta^2H_{c\text{-signal}}$ (Lehmann et al., 2021b).

Deciduous ring-porous species like *Quercus* partly rely on stored photosynthates for earlywood growth (Pilcher and Frenzel, 1995), resulting in mixed climatic information from previous years and the current growing season (Reynolds-Henne et al., 2009). In our study, we reduced the potential effect of storage remobilization by sampling only the latewood of *Quercus* (Waterhouse et al., 2002). This strategy was successful for the $\delta^{18}O_{c\text{-signal}}$, which showed high correlation values (Fig. 3), especially at the British sites (Rinne et al., 2013), but it did not seem effective for the $\delta^2H_{c\text{-signal}}$, which exhibited low ones. It should be considered that storage use could still play a role under stressful conditions even for late-wood growth (Sarris et al., 2013) However, other yet to be characterized isotope fractionations may likely interfere autonomously with the current-year $\delta^2H_{c\text{-signal}}$ in *Quercus* (e.g. growth release: Lehmann et al., 2021b).

On the contrary, *Pinus* relies largely on fresh (current-year) photosynthates as the main source for tree-ring production (Dickmann and Kozlowski, 1970) in temperate sites and under non-drought conditions. A large photosynthetic demand and high transpiration rate ensure a fast turnover of leaf-water in *Pinus* and, therefore, a reliable recording of the seasonal climate signals (Dickmann and Kozlowski, 1970; Glerum, 1980), as confirmed by our results (Fig. 3).

4.3.2. Root system and source water interactions

Water from different soil layers systematically varies in its isotopic composition. The topsoil is directly dependent on precipitation events and subject to evaporative isotopic enrichment, thus recording current-year climatic signals. On the contrary, the isotopic composition of deeper soil layers is also dependent on winter precipitation and snow melt, and therefore previous years' climate (Allen et al., 2019). Since no isotopic fractionation typically occurs during root-water uptake (Dawson and Siegwolf, 2007; Geris et al., 2015; Tang et al., 2000), the xylem water (also known as source water) integrated during tree-ring cellulose formation (Augusti et al., 2006; Roden and Ehleringer, 2000) can reflect the uptake depth of soil water. The typical genus-specific rooting depth therefore influences the $\delta^2H_{c\text{-signal}}$. Shallow-rooted *Pinus* generally carries a stronger current-year climate signal, because its source water mostly integrates precipitation events (Fig. 3), as previously shown for other shallow-rooted species (Tang and Feng, 2001). On the contrary, *Quercus* xylem water has been shown to carry a deep-soil signal or a mixture between deep and shallow soil (Barbeta et al., 2020), hence diluting its precipitation-induced $\delta^2H_{c\text{-signal}}$. However, *Quercus* was reported to use current-year precipitation in clay-rich soil, (e.g. WOB site: Rinne et al., 2013), stressing once again the site-specificity of $\delta^2H_{c\text{-signal}}$.

While the different rooting depths can explain the stronger $\delta^2H_{c\text{-signal}}$ for *Pinus* than for *Quercus*, the decoupling of H-$O_{\text{-signal}}$ at the drier and warmer sites remains unexplained (Fig. 5). A growing number of studies have suggested that isotope fractionations can occur during root water uptake (Evaristo et al., 2017; Oerter et al., 2019), as δ^2H in stem water has been observed to be progressively enriched with increasing transpiration while $\delta^{18}O$ still reflected the soil water isotopic signal (Barbeta et al., 2020; Ellsworth and Williams, 2007). This mismatch between δ^2H and $\delta^{18}O$ in xylem water could further depend on multiple interacting factors, such as (i) the heterogeneity within the soil matrix (Oerter et al., 2014); (ii) isotope separation between bound and mobile soil water (Tang and Feng, 2001);

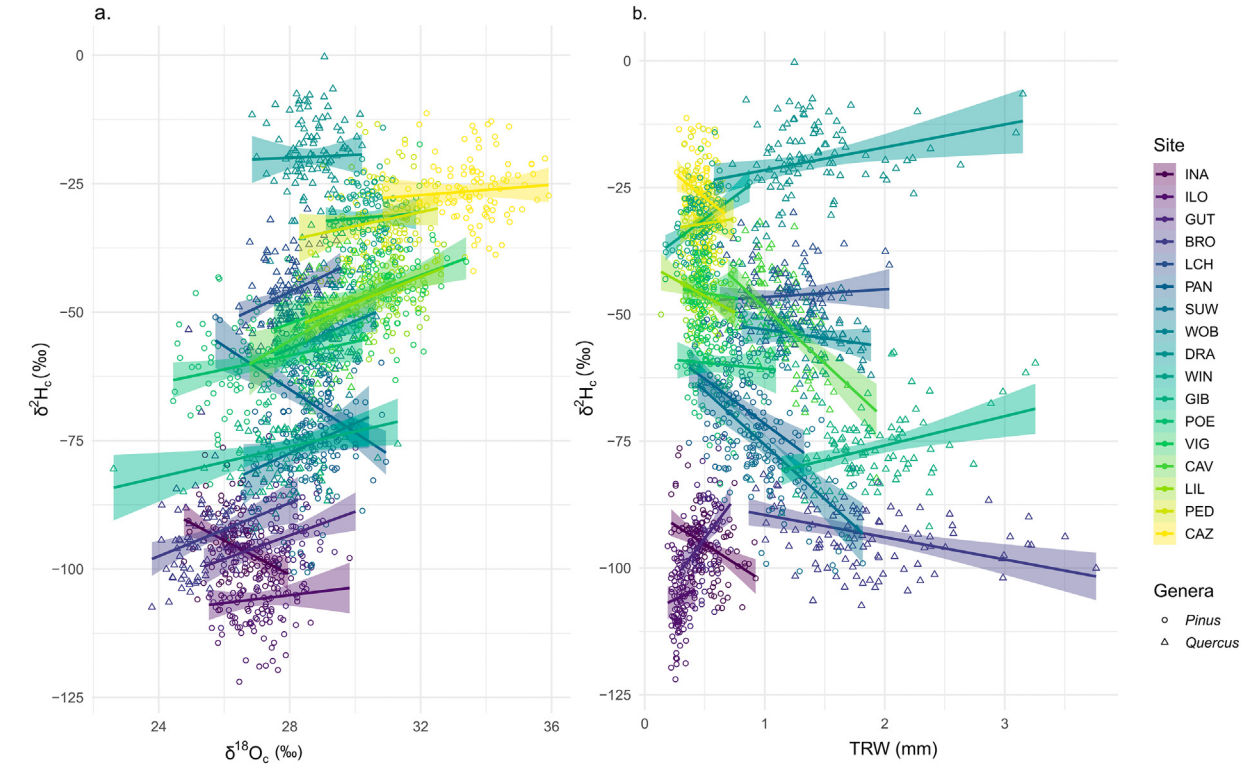

Fig. 7. Linear relationships between (a) δ^2H_c and $\delta^{18}O_c$, and (b) δ^2H_c and TRW for each site. See Fig. S.7 for the same relationships but with FDiff data. The fitted linear model equations, explained variance (r^2), and significance (*p*-values) are given in Table S.5. Pearson's correlation coefficients (r) calculated for δ^2H_c and $\delta^{18}O_c$ and for δ^2H_c and TRW are given in Fig. S.6.

(iii) root interactions with water pools, and isotope compartmentalization (Zhao et al., 2016); and (iv) methodological artefacts (Chen et al., 2020), which could explain the decoupling of $H\text{-}O_{\text{-signal}}$ between the two genera.

Based on our results, we conclude that the δ^2H_c of *Pinus* is a more sensitive indicator of environmental changes than the δ^2H_c of *Quercus*, although further research is needed to investigate the driving factors of these species' differences.

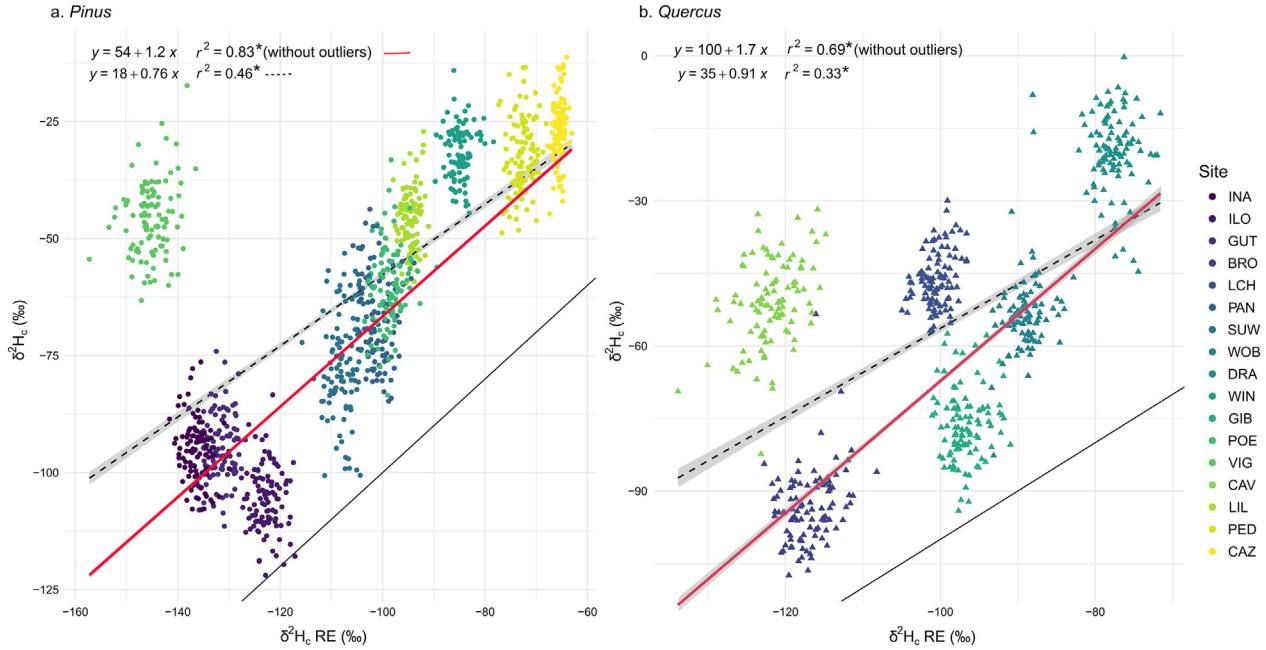

Fig. 8. Relationship between measured (δ^2H_c) and modelled (δ^2H_c RE) values of δ^2H_c chronologies for *Pinus* (a) and *Quercus* (b). Linear regressions were fitted for all sites (black dotted lines), and for all sites without the outlier sites VIG and CAV (red solid lines). Significance is indicated by asterisks * ($P < 0.05$). The 1:1 line is indicated by a black solid line. Results of genera-specific regressions are given in Table S.6. See Fig. S.7 for the same relationships but with FDiff data. (For interpretation of the references to colour in this figure legend, the reader is referred to the web version of this article.)

4.3.3. Influence of extreme wet and dry summer conditions

We hypothesized that years with extreme wet or dry summer conditions, ergo with contrasting VPD and precipitation conditions, lead to distinct ecophysiological responses that shape $\delta^2H_{c\text{-signal}}$ (**Hp1c**). Climatic conditions induce changes in the isotopic composition typically leading to higher δ^2H values of leaf and source water in dry years compared with normal years, and lower values in wet years. These patterns should subsequently be imprinted on δ^2H_c (Cernusak et al., 2016; Roden and Ehleringer, 2000). We indeed observed a significant ^2H-enrichment in tree rings of both genera in dry years compared with normal years, but not a clear ^2H-depletion in wet years (Fig. 6). This was unforeseen because the climatic signal transfer from the water isotopes to the tree rings was expected to be more consistent under wet conditions than dry conditions because of an increased translocation of recent photosynthates towards the stem cambium (Michelot et al., 2012b; Pflug et al., 2015; Simard et al., 2013). The general ^2H-enrichment in tree-ring cellulose under dry conditions thus does not necessarily reflect a climatic signal derived from changes in the isotopic composition of water. It might rather be derived from drought-driven changes in metabolic pathways (Cormier et al., 2018) or from greater use of (potentially ^2H-enriched) carbohydrate reserves for wood formation under stress conditions (Lehmann et al., 2021a).

Therefore, in contrast to our hypothesis (**Hp1c**) that expected differences between the two genera based on their contrasting ecophysiological traits which affect leaf and source water isotope modification in response to drought (Klein, 2014; Martín-Gómez et al., 2017), both *Quercus* and *Pinus* showed ^2H-enrichment in dry years compared with normal years. Our results provide novel evidence that δ^2H_c values might function as an indicator for extreme drought conditions, potentially due to specific ^2H-fractionations that are only triggered under reduced water availability. However, additional δ^2H_c studies focusing on drought effects are needed to further understand the potential of δ^2H_c as a drought proxy.

4.4. Disentangling the hydrological and physiological information in δ^2H_c

To fully understand the nature of the δ^2H_c information recorded in tree rings, it is necessary to quantify the individual impacts of climatic, hydrological, and physiological factors. Therefore, we evaluated the relationship of δ^2H_c chronologies with those of $\delta^{18}O_c$ and TRW, and the performance of the mechanistic model in estimating δ^2H_c in tree rings.

4.4.1. Relationship between δ^2H_c and $\delta^{18}O_c$ and between δ^2H_c and TRW

The hydrological and temperature signals are recorded by δ^2H_c and $\delta^{18}O_c$ at a continental scale (Gray and Song, 1984; Saurer et al., 1997b), as shown by their distribution along the global meteoric water line (Fig. S.9). Our results indicate that $\delta^{18}O$ transfers the source water signal to the tree rings better than δ^2H, resulting in a stronger climate signal (Fig. 3). However, the well-known relationship between the two water isotopes in hydrological cycles barely hold for the year-to-year variation in tree-ring cellulose, as shown by the weak relationships between the δ^2H_c and $\delta^{18}O_c$ chronologies for most of our studied sites, regardless of species and geographical location (Fig. 7a). This result is likely caused by temporal variability in fractionations and additional factors that influence ^2H-fractionations more than ^{18}O-fractionations. However, the climatic and hydrological information that dominates $\delta^{18}O_c$ is likely also present, albeit weakly, in δ^2H_c. The magnitude of δ^2H_c may depend on site-specific precipitation and temperature conditions, as indicated by the positive influence of MP_{JJA} and negative influence of MT_{JJA} on the δ^2H_c–$\delta^{18}O_c$ relationships (Fig. S.8) (Sprenger et al., 2016).

Trees' physiological strategies in response to the local environment are recorded partly by TRW (Hartl-Meier et al., 2015), and thus the δ^2H_c–TRW relationships should reflect shared physiological information. Indeed, our δ^2H_c–TRW relationships were stronger than δ^2H_c–$\delta^{18}O_c$ relationships at many sites (Fig. 7b). This supports that at many sites the δ^2H_c recorded a stronger physiological signal rather than a climatic or hydrological one as proposed in our second hypothesis (**Hp2**). Whereas in most cases a significant negative TRW-δ^2H_c relationship was found in our study, a few significant positive relationships also appeared (Fig. S.6). Although neither positive nor negative relationships clustered in a particular geographical area, or in distinct climatic regions, we observed a negative influence of MT_{JJA} on the slope of the δ^2H_c–TRW relationship (Fig. S.8). Lehmann et al. (2021b) reported that negative δ^2H_c-TRW relationships indicate greater use of carbohydrate storage under stress conditions at four sites in Europe and Asia, where growth was limited by precipitation or light. On the contrary, at a site where temperature was the growth-limiting factor, the δ^2H_c-TRW relationship became positive. Nonetheless, this uneven share of negative (7) and positive (4) relationships between δ^2H_c and TRW suggests that stronger site-specific variables, like stand density or soil depth, are needed to advance our understanding of δ^2H_c variations.

4.4.2. Performance of the mechanistic RE-model

The mechanistic RE-model was previously found to successfully explain the δ^2H_c of young broadleaf trees (*Alnus incana*, *Betula occidentalis* and *Populus fremontii*) under controlled experimental conditions (Roden et al., 2000). However, its applicability across a variety of species and ecological conditions was not originally tested. Our δ^2H_c simulations produced using the RE-model support our last hypothesis (**Hp3**). We observed a reasonable δ^2H_c simulation values for both genera on a continental scale, albeit with an overall consistent overestimation (Fig. 8). This suggests that the RE-model successfully takes into account the large-scale isotopic variations in precipitation, while the constant overestimation may be attributed to a lack of dilution effects (e.g. Péclet effect or two-pool estimations) in the CG-model to estimate δ^2H_{lw} (Roden et al., 2015). Therefore, species-specific and temporally variable dilution effects should be considered in future studies (Voelker et al., 2014).

As hypothesized (**Hp3**), the modelled δ^2H_c data did not capture the site-specific inter-annual variability, as shown by both δ^2H_c and FDiff δ^2H_c data (Figs. 8, S.7). Several sources of uncertainty should be considered to evaluate the performance of the RE-model. First, the low spatial resolution of the gridded climate data available for the last century. For example, the two Swiss sites located at different elevations (CAV and VIG) share the same climatic information, leading to a larger overestimation of the δ^2H_c values at the higher-elevation *Pinus* site (VIG). Second, the lack of annual site-level δ^2H precipitation data (used as source water) and unknown mixing effects of the precipitation water with ground water also play a role (Waterhouse et al., 2002). Third, the model does not account for the stochasticity of environmental parameters, such as temperature, that may influence biochemical isotope fractionation (Zhou et al., 2011). Finally, the species differences in ^2H-fractionation (Arosio et al., 2020b) are not considered in mechanistic models.

We observed that modelled δ^2H_c has a better fit with measured *Pinus* δ^2H_c than measured *Quercus* δ^2H_c at continental scale (Fig. 8). These results corroborate previous findings that the isotopic signature of precipitation is better captured in the δ^2H_c of shallow-rooted (*Pinus*) than deep-rooted (*Quercus*) trees, due to their ability to access deeper groundwater (Voelker et al., 2014; Waterhouse et al., 2002). Our results clearly demonstrate the necessity to take into account species-specific or functional-trait-dependent (Arosio et al., 2020b; Cormier et al., 2018; Sanchez-Bragado et al., 2019), as well as age-dependent weighting factors (Arosio et al., 2020a). These additions would account for the non-controlled conditions of natural forests and should be integrated into future mechanistic models.

4.5. Potential and limitations of δ^2H_c chronologies

In this study we demonstrate that δ^2H_c chronologies record a mix of hydrological and climatic signals, while the physiological information is still not readily accessible, due to remaining gaps in the understanding of ^2H-fractionations and their interactions with C partitioning mechanisms, and with climatological, hydrological processes (Waterhouse et al., 2002). New high-throughput methods will make δ^2H_c measurements increasingly accessible and economically viable (Filot et al., 2006; Sauer et al., 2009; Wassenaar et al., 2015), which will likely

boost the knowledge on ^{2}H-fractionations in plants in the next years. Thus, further targeted research to disentangle the interference of climatic and metabolic signals is needed, carried out in well-monitored forest sites or in growth chambers with controlled conditions. This untapped physiological signal in $\delta^{2}H_c$ could lead to further insight into carbohydrate storage use, drought stress, and carbon allocation processes, information that is useful not only from a retrospective view, but also for improving growth models and thus predicting future tree performance.

5. Conclusions

The results presented here set a baseline in the understanding of the information stored in $\delta^{2}H_c$. We show that the climate information recorded by $\delta^{2}H_c$ is weaker than for $\delta^{13}C_c$ and $\delta^{18}O_c$, and that it is site and genera dependent, with *Pinus* showing a stronger climatic signal than *Quercus*. Thus, information recorded by $\delta^{2}H_c$ is different from that of $\delta^{13}C_c$ and $\delta^{18}O_c$, with a stronger physiological component independent from climate, although these effects cannot yet be disentangled. As shown by our results, these physiological effects are significant, but not constant across years, sites, or genera. Nonetheless, years with dry summer conditions showed a consistent ^{2}H-enrichemnt for both genera. Therefore, combination with other tree-ring-derived parameters is highly advisable to provide complementary information on tree performance. Finally, we showed that the current mechanistic $\delta^{2}H_c$ models performed well at a continental but not at a temporal scale. Clearly, improved climate and source water data, as well as further work on mechanistic isotope models is need to improve the spatio-temporal estimation of $\delta^{2}H_c$. This will eventually result in tree rings $\delta^{2}H_c$ to be a highly valuable archive of how trees' physiology and biochemistry has been influenced by past environmental changes.

Funding

This study was supported by the ISONET EU-project (EVK-CT-2002-00147):

ML: SNF projects 103829, 107554, 111699, and 116540 for the work at the University of Bern.

VV, MS: SNF project 200020_182092.

EMS and KT: SNF project TRoxy (No. 200021_175888).

ID-L: Fundació La Caixa through the Junior Leader Program (LCF/BQ/LR18/11640004).

NJL: NERC (NE/P011527/1) and SSHRC (895-2019-1015).

KRG: ERC (755865) and Academy of Finland (295319).

EG: Spanish Ministerio de Educación y Ciencia project REN2002-11476-E/CLI.

MML: SNF Ambizione project TreeCarbo (No. 179978).

CRedit authorship contribution statement

VV completed the data analyses and wrote the first manuscript draft with MS and MML. The manuscript was further developed with the help of EMS and KT. Data were provided by MS, KT, KRG, ML, NJL, and STA. All authors contributed to the writing of the manuscript and agreed upon the final version.

Declaration of competing interest

The authors declare that they have no known competing financial interests or personal relationships that could have appeared to influence the work reported in this paper.

Acknowledgements

We acknowledge Nyfeler P. and Moret H., as well as Filot M., for developing the online equilibration system and performing measurements at the University of Bern, Switzerland. We thank Rolfe J. and Hall M. (Godwin Laboratory, UK) for technical support. We are grateful to Muntán E., Bosch O., and Planells O., from the Department of Ecology, UB. Spain, who helped us with field and laboratory work. We thank Grinsted M.J. and Wilson A.T. for inspiring model ideas.

Appendix A. Supplementary data

Supplementary data to this article can be found online at https://doi.org/10.1016/j.scitotenv.2021.152281.

References

Allen, S.T., Kirchner, J.W., Braun, S., Siegwolf, R.T.W., Goldsmith, G.R., 2019. Seasonal origins of soil water used by trees. Hydrol. Earth Syst. Sci. 23 (2), 1199–1210.

An, W., Liu, X., Leavitt, S.W., Xu, G., Zeng, X., Wang, W., et al., 2014. Relative humidity history on the batang-litang plateau of western China since 1755 reconstructed from tree-ring δ18O and δD. Clim. Dyn. 42 (9–10), 2639–2654.

Andreu-Hayles, L., Planells, O., Gutiérrez, E., Muntan, E., Helle, G., Anchukaitis, K.J., et al., 2011. Long tree-ring chronologies reveal 20th century increases in water-use efficiency but no enhancement of tree growth at five iberian pine forests. Glob. Chang. Biol. 17 (6), 2095–2112.

Andreu-Hayles, L., Ummenhofer, C.C., Barriendos, M., Schleser, G.H., Helle, G., Leuenberger, M., et al., 2017. 400 years of summer hydroclimate from stable isotopes in iberian trees. Clim. Dyn. 49 (1–2), 143–161.

Anhäuser, T., Sehls, B., Thomas, W., Hartl, C., Greule, M., Scholz, D., et al., 2020. Tree-ring δ2H values from lignin methoxyl groups indicate sensitivity to european-scale temperature changes. Palaeogeogr. Palaeoclimatol. Palaeoecol. 546, 109665.

Aranda, I., Gil, L., Pardos, J.A., 2000. Water relations and gas exchange in Fagus sylvatica L. and Quercus petraea (Mattuschka) liebl. in a mixed stand at their southern limit of distribution in Europe. Trees 14 (6), 344–352.

Arosio, T., Ziehmer-Wenz, M.M., Nicolussi, K., Schlüchter, C., Leuenberger, M., 2020a. Cambial-age related correlations of stable isotopes and tree-ring widths in wood samples of tree-line conifers. Biogeosci. Discuss. https://doi.org/10.5194/bg-2020-406 [preprint].

Arosio, T., Ziehmer-Wenz, M.M., Nicolussi, K., Schlüchter, C., Leuenberger, M., 2020. Larch cellulose shows significantly depleted hydrogen isotope values with respect to evergreen conifers in contrast to oxygen and carbon isotopes. Front. Earth Sci. 8.

Augusti, A., Betson, T.R., Schleucher, J., 2006. Hydrogen exchange during cellulose synthesis distinguishes climatic and biochemical isotope fractionations in tree rings. New Phytol. 172 (3), 490–499.

Balting, D.F., Ionita, M., Wegmann, M., Helle, G., Schleser, G.H., Rimbu, N., et al., 2021. Large-scale climate signals of a european oxygen isotope network from tree rings. Clim. Past 17 (3), 1005–1023.

Barbeta, A., Gimeno, T.E., Clavé, L., Fréjaville, B., Jones, S.P., Delvigne, C., et al., 2020. An explanation for the isotopic offset between soil and stem water in a temperate tree species. New Phytol. 227 (3), 766–779.

Barbour, M.M., Walcroft, A.S., Farquhar, G.D., 2002. Seasonal variation in δ13C and δ18O of cellulose from growth rings of Pinus radiata. Plant Cell Environ. 25 (11), 1483–1499.

Boettger, T., Haupt, M., Knöller, K., Weise, S.M., Waterhouse, J.S., Rinne, K.T., et al., 2007. Wood cellulose preparation methods and mass spectrometric analyses of δ13C and δ18O, and nonexchangeable δ2H values in cellulose, sugar, and starch: an interlaboratory comparison. Anal. Chem. 79 (12), 4603–4612.

Boettger, T., Haupt, M., Friedrich, M., Waterhouse, J.S., 2014. Reduced climate sensitivity of carbon, oxygen and hydrogen stable isotope ratios in tree-ring cellulose of silver fir (Abies alba Mill.) influenced by background SO2 in Franconia (Germany, Central Europe). Environ. Pollut. (Barking, Essex 1987) 185, 281–294.

Bowen, G.J., 2008. Spatial analysis of the intra-annual variation of precipitation isotope ratios and its climatological corollaries. J. Geophys. Res. 113 (D5), 1–10.

Bréda, N., Badeau, V., 2008. Forest tree responses to extreme drought and some biotic events: towards a selection according to hazard tolerance? Compt. Rendus Geosci. 340 (9–10), 651–662.

Bréda, N., Cochard, H., Dreyer, E., Granier, A., 1993. Field comparison of transpiration, stomatal conductance and vulnerability to cavitation of Quercus petraea and Quercus robur under water stress. Ann. For. Sci. 50 (6), 571–582.

Bréda, N., Huc, R., Granier, A., Dreyer, E., 2006. Temperate forest trees and stands under severe drought: a review of ecophysiological responses, adaptation processes and long-term consequences. Ann. For. Sci. 63 (6), 625–644.

Brooks, R.J., Barnard, H.R., Coulombe, R., McDonnell, J.J., 2010. Ecohydrologic separation of water between trees and streams in a Mediterranean climate. Nat. Geosci. 3 (2), 100–104.

Cernusak, L.A., Farquhar, G.D., Pate, J.S., 2005. Environmental and physiological controls over oxygen and carbon isotope composition of Tasmanian blue gum Eucalyptus globulus. Tree Physiol. 25 (2), 129–146.

Cernusak, L.A., Barbour, M.M., Arndt, S.K., Cheesman, A.W., English, N.B., Feild, T.S., et al., 2016. Stable isotopes in leaf water of terrestrial plants. Plant Cell Environ. 39 (5), 1087–1102.

Cheesman, A.W., Cernusak, L.A., 2017. Infidelity in the outback: climate signal recorded in Δ18O of leaf but not branch cellulose of eucalypts across an australian aridity gradient. Tree Physiol. 37 (5), 554–564.

Chen, Y., Helliker, B.R., Tang, X., Li, F., Zhou, Y., Song, X., 2020. Stem water cryogenic extraction biases estimation in deuterium isotope composition of plant source water. Proc. Natl. Acad. Sci. U. S. A. 117 (52), 33345–33350.

Christiansen, B., Ljungqvist, F.C., 2017. Challenges and perspectives for large-scale temperature reconstructions of the past two millennia. Rev. Geophys. 55 (1), 40–96.
Cook, E.R., Kairiukstis, L.A., 1990. Methods of Dendrochronology: Applications in the Environmental Sciences. Springer Netherlands, Dordrecht.
Cormier, M.-A., Werner, R.A., Sauer, P.E., Gröcke, D.R., Leuenberger, M.C., Wieloch, T., et al., 2018. 2H-fractionations during the biosynthesis of carbohydrates and lipids imprint a metabolic signal on the δ2H values of plant organic compounds. New Phytol. 218 (2), 479–491.
Craig, H., 1961. Isotopic variations in meteoric waters. Science (New York, N.Y.) 133 (3465), 1702–1703.
Craig, H., Gordon, I., 1965. I. Deuterium and oxygen 18 variations in the ocean and the marine atmosphere. Stable Isotopes in Oceanographic Studies and Paleotemperatures: Consiglio nazionale delle richerche, Laboratorio di geologia nucleare.
Dansgaard, W., 1964. Stable isotopes in precipitation. Tellus 16 (4), 436–468.
Dawson, T.E., Siegwolf, R.T.W. (Eds.), 2007. Stable Isotopes as Indicators of Ecological Change. Academic, Oxford.
Dickmann, D.I., Kozlowski, T.T., 1970. Mobilization and incorporation of photoassimilated C by growing vegetative and reproductive tissues of adult Pinus resinosa ait. trees. Plant Physiol. 45 (3), 284–288.
Dongmann, G., Nürnberg, H.W., Förstel, H., Wagener, K., 1974. On the enrichment of H2 18O in the leaves of transpiring plants. Radiat. Environ. Biophys. 11 (1), 41–52.
Dunbar, J., Schmidt, H.-L., 1984. Measurement of the 2H/1H ratios of the carbon bound hydrogen atoms in sugars. Fresenius' Z. Anal. Chem. 317 (857), 853.
Edwards, T., Fritz, P., 1986. Assessing meteoric water composition and relative humidity from18O and2H in wood cellulose: paleoclimatic implications for southern Ontario, Canada. Appl. Geochem. 1 (6), 715–723.
Ellsworth, P.Z., Williams, D.G., 2007. Hydrogen isotope fractionation during water uptake by woody xerophytes. Plant Soil 291 (1–2), 93–107.
Epstein, S., Yapp, C.J., 1976. Climatic implications of the D/H ratio of hydrogen in C-H groups in tree cellulose. Earth Planet. Sci. Lett. 30, 252–261.
Esper, J., Frank, D.C., Battipaglia, G., Büntgen, U., Holert, C., Treydte, K., et al., 2010. Low-frequency noise in δ13C and δ18O tree ring data: a case study of Pinus uncinata in the spanish Pyrenees. Glob. Biogeochem. Cycles 24 (4) (n/a-n/a).
Etien, N., Daux, V., Masson-Delmotte, V., Mestre, O., Stievenard, M., Guillemin, M.T., et al., 2009. Summer maximum temperature in northern France over the past century: instrumental data versus multiple proxies (tree-ring isotopes, grape harvest dates and forest fires). Clim. Chang. 94 (3–4), 429–456.
Evaristo, J., McDonnell, J.J., Clemens, J., 2017. Plant source water apportionment using stable isotopes: a comparison of simple linear, two-compartment mixing model approaches. Hydrol. Process. 31 (21), 3750–3758.
Feng, X., Epstein, S., 1994. Climatic implications of an 8000-year hydrogen isotope time series from bristlecone pine trees. Science (New York, N.Y.) 265 (5175), 1079–1081.
Filot, M.S., Leuenberger, M., Pazdur, A., Boettger, T., 2006. Rapid online equilibration method to determine the D/H ratios of non-exchangeable hydrogen in cellulose. Rapid Commun. Mass Spectrom. 20 (22), 3337–3344.
Frank, D.C., Poulter, B., Saurer, M., Esper, J., Huntingford, C., Helle, G., et al., 2015. Water-use efficiency and transpiration across european forests during the anthropocene. Nature Clim Change 5 (6), 579–583.
Geris, J., Tetzlaff, D., McDonnell, J., Anderson, J., Paton, G., Soulsby, C., 2015. Ecohydrological separation in wet, low energy northern environments? A preliminary assessment using different soil water extraction techniques. Hydrol. Process. 29 (25), 5139–5152.
Gessler, A., Ferrio, J.P., Hommel, R., Treydte, K., Werner, R.A., Monson, R.K., 2014. Stable isotopes in tree rings: towards a mechanistic understanding of isotope fractionation and mixing processes from the leaves to the wood. Tree Physiol. 34 (8), 796–818.
Giuggiola, A., Ogée, J., Rigling, A., Gessler, A., Bugmann, H., Treydte, K., 2016. Improvement of water and light availability after thinning at a xeric site: which matters more? A dual isotope approach. New Phytol. 210 (1), 108–121.
Glerum, C., 1980. Food sinks and food reserves of trees in temperate climates. N. Z. J. For. Sci. 176–185.
Gori, Y., Wehrens, R., Greule, M., Keppler, F., Ziller, L., La Porta, N., et al., 2013. Carbon, hydrogen and oxygen stable isotope ratios of whole wood, cellulose and lignin methoxyl groups of Picea abies as climate proxies. Rapid Commun. Mass Spectrom. 27 (1), 265–275.
Gray, J., Song, S.J., 1984. Climatic implications of the natural variations of D/H ratios in tree ring cellulose. Earth Planet. Sci. Lett. 70 (1), 129–138.
Green, J.W., 1963. Wood cellulose. In: Whistler, R.L. (Ed.), Methods in Carbohydrate Chemistry.
Grossiord, C., Gessler, A., Granier, A., Berger, S., Bréchet, C., Hentschel, R., et al., 2014. Impact of interspecific interactions on the soil water uptake depth in a young temperate mixed species plantation. J. Hydrol. 519, 3511–3519.
Guerrieri, R., Belmecheri, S., Ollinger, S.V., Asbjornsen, H., Jennings, K., Xiao, J., et al., 2019. Disentangling the role of photosynthesis and stomatal conductance on rising forest water-use efficiency. Proc. Natl. Acad. Sci. U. S. A. 116 (34), 16909–16914.
Hafner, P., Robertson, I., McCarroll, D., Loader, N.J., Gagen, M., Bale, R.J., et al., 2011. Climate signals in the ring widths and stable carbon, hydrogen and oxygen isotopic composition of Larix decidua growing at the forest limit in the southeastern european Alps. Trees 25 (6), 1141–1154.
Harris, I., Osborn, T.J., Jones, P., Lister, D., 2020. Version 4 of the CRU TS monthly high-resolution gridded multivariate climate dataset. Sci. Data 7 (1), 109.
Hartl-Meier, C., Zang, C., Büntgen, U., Esper, J., Rothe, A., Göttlein, A., et al., 2015. Uniform climate sensitivity in tree-ring stable isotopes across species and sites in a mid-latitude temperate forest. Tree Physiol. 35 (1), 4–15.
Haupt, M., Weigl, M., Grabner, M., Boettger, T.A., 2011. 400-year reconstruction of july relative air humidity for the Vienna region (eastern Austria) based on carbon and oxygen stable isotope ratios in tree-ring latewood cellulose of oaks (Quercus petraea Matt. Liebl.). Clim. Chang. 105 (1–2), 243–262.
Helle, G., Schleser, G.H., 2004. Beyond CO2-fixation by rubisco - an interpretation of 13C/12C variations in tree rings from novel intra-seasonal studies on broad-leaf trees. Plant Cell Environ. 27 (3), 367–380.
Hilasvuori, E., Berninger, F., 2010. Dependence of tree ring stable isotope abundances and ring width on climate in finnish oak. Tree Physiol. 30 (5), 636–647.
Hochberg, U., Rockwell, F.E., Holbrook, N.M., Cochard, H., 2018. Iso/Anisohydry: a plant-environment interaction rather than a simple hydraulic trait. Trends Plant Sci. 23 (2), 112–120.
Holmes, R., 1983. Computer-assisted quality control in tree-ring dating and measurement. Tree-Ring Bull. 43, 69–78.
Irvine, J., Perks, M.P., Magnani, F., Grace, J., 1998. The response of Pinus sylvestris to drought: stomatal control of transpiration and hydraulic conductance. Tree Physiol. 18 (6), 393–402.
Joussaume, S., Jouzel, J., 1993. Paleoclimatic tracers: an investigation using an atmospheric general circulation model under ice age conditions: 2. Water isotopes. J. Geophys. Res. 98 (D2), 2807–2830.
Kimak, A., 2015. Tracing Physiological Processes of Long Living Tree Species and Their Response on Climate Change Using Triple Isotope Analyses.
Kimak, A., Leuenberger, M., 2015. Are carbohydrate storage strategies of trees traceable by early–latewood carbon isotope differences? Trees 29 (3), 859–870.
Kimak, A., Kern, Z., Leuenberger, M., 2015. Qualitative distinction of autotrophic and heterotrophic processes at the leaf level by means of triple stable isotope (C-O-H) patterns. Front. Plant Sci. 6, 1008.
Klein, T., 2014. The variability of stomatal sensitivity to leaf water potential across tree species indicates a continuum between isohydric and anisohydric behaviours. Funct. Ecol. 28 (6), 1313–1320.
Klesse, S., Weigt, R., Treydte, K.S., Saurer, M., Schmid, L., Siegwolf, R.T., et al., 2018. Oxygen isotopes in tree rings are less sensitive to changes in tree size and relative canopy position than carbon isotopes. Plant Cell Environ. 41 (12), 2899–2914.
Laitakari, E., 1927. Morphological study of scots pine root system. Acta For. Fenn. 33 (1).
Lavergne, A., Voelker, S., Csank, A., Graven, H., de Boer, H.J., Daux, V., et al., 2020. Historical changes in the stomatal limitation of photosynthesis: empirical support for an optimality principle. New Phytol. 225 (6), 2484–2497.
Lehmann, M.M., Goldsmith, G.R., Schmid, L., Gessler, A., Saurer, M., Siegwolf, R.T.W., 2018. The effect of 18 O-labelled water vapour on the oxygen isotope ratio of water and assimilates in plants at high humidity. New Phytol. 217 (1), 105–116.
Lehmann, M.M., Schuler, P., Cormier, M.-A., Allen, S.T., Leuenberger, M., Voelker, S., 2021a. Chapter: the stable hydrogen isotopic signature: from source water to tree rings. Stable Isotopes in Tree Rings: Inferring Physiological, Climatic and Environmental Responses in print.
Lehmann, M.M., Vitali, V., Schuler, P., Leuenberger, M., Saurer, M., 2021b. More than climate: hydrogen isotope ratios in tree rings as novel plant physiological indicator for stress conditions. Dendrochronologia 65, 125788.
Leo, M., Oberhuber, W., Schuster, R., Grams, T.E.E., Matyssek, R., Wieser, G., 2014. Evaluating the effect of plant water availability on inner alpine coniferous trees based on sap flow measurements. Eur. J. For. Res. 133 (4), 691–698.
Levesque, M., Andreu-Hayles, L., Smith, W.K., Williams, A.P., Hobi, M.L., Allred, B.W., et al., 2019. Tree-ring isotopes capture interannual vegetation productivity dynamics at the biome scale. Nat. Commun. 10 (1), 742.
Lipp, J., Trimborn, P., Fritz, P., Moser, H., Becker, B., Frenzel, B., 1991. Stable isotopes in tree ring cellulose and climatic change. Tellus Ser. B Chem. Phys. Meteorol. 43 (3), 322–330.
Loader, N.J., Gagen, M., Robertson, I., Jalkanen, R., McCarroll, D., 2007. Extracting climatic information from stable isotopes in tree rings. In: Dawson, T.E., Siegwolf, R.T.W. (Eds.), Stable Isotopes as Indicators of Ecological Change. Academic, Oxford, pp. 25–48.
Loader, N.J., Santillo, P.M., Woodman-Ralph, J.P., Rolfe, J.E., Hall, M.A., Gagen, M., et al., 2008. Multiple stable isotopes from oak trees in southwestern Scotland and the potential for stable isotope dendroclimatology in maritime climatic regions. Chem. Geol. 252 (1–2), 62–71.
Loader, N.J., Young, G., Grudd, H., McCarroll, D., 2013. Stable carbon isotopes from Torneträsk, northern Sweden provide a millennial length reconstruction of summer sunshine and its relationship to Arctic circulation. Quat. Sci. Rev. 62, 97–113.
Loader, N.J., Young, G.H.F., McCarroll, D., Davies, D., Miles, D., Bronk, Ramsey C., 2020. Summer precipitation for the England and Wales region, 1201–2000 ce from stable oxygen isotopes in oak tree rings. J. Quat. Sci. 35 (6), 731–736.
Luo, Y., Sternberg, L.D.S.L., 1992. Hydrogen and oxygen isotopic fractionation during heterotrophic cellulose synthesis. J. Exp. Bot. 43 (1), 47–50.
Majoube, M., 1971. Fractionnement en oxygène 18 et en deutérium entre l'eau et sa vapeur. J. Chim. Phys. 68, 1423–1436.
Martínez-Sancho, E., Dorado-Liñán, I., Gutiérrez Merino, E., Matiu, M., Helle, G., Heinrich, I., et al., 2018. Increased water-use efficiency translates into contrasting growth patterns of scots pine and sessile oak at their southern distribution limits. Glob. Chang. Biol. 24 (3), 1012–1028.
Martín-Gómez, P., Aguilera, M., Pemán, J., Gil-Pelegrín, E., Ferrio, J.P., 2017. Contrasting ecophysiological strategies related to drought: the case of a mixed stand of scots pine (Pinus sylvestris) and a submediterranean oak (Quercus subpyrenaica). Tree Physiol. 37 (11), 1478–1492.
Mayr, C., Frenzel, B., Friedrich, M., Spurk, M., Stichler, W., Trimborn, P., 2003. Stable carbon- and hydrogen-isotope ratios of subfossil oaks in southern Germany: methodology and application to a composite record for the holocene. The Holocene 13 (3), 393–402.
Merlin, M., Perot, T., Perret, S., Korboulewsky, N., Vallet, P., 2015. Effects of stand composition and tree size on resistance and resilience to drought in sessile oak and scots pine. For. Ecol. Manag. 339, 22–33.
Merlivat, L., 1978. Molecular diffusivities of $H^2\,^{16}O$, $HD^{16}O$, and $H^2\,^{18}O$ in gases. J. Chem. Phys. 69 (6), 2864.
Michelot, A., Bréda, N., Damesin, C., Dufrêne, E., 2012a. Differing growth responses to climatic variations and soil water deficits of Fagus sylvatica, Quercus petraea and Pinus sylvestris in a temperate forest. For. Ecol. Manag. 265, 161–171.

Michelot, A., Simard, S., Rathgeber, C., Dufrêne, E., Damesin, C., 2012b. Comparing the intra-annual wood formation of three european species (Fagus sylvatica, Quercus petraea and Pinus sylvestris) as related to leaf phenology and non-structural carbohydrate dynamics. Tree Physiol. 32 (8), 1033–1045.
Murray, F.W., 1967. On the computation of saturation vapor pressure. J. Appl. Meteor. 6 (1), 203–204.
Nabeshima, E., Nakatsuka, T., Kagawa, A., Hiura, T., Funada, R., 2018. Seasonal changes of δD and δ18O in tree-ring cellulose of Quercus crispula suggest a change in post-photosynthetic processes during earlywood growth. Tree Physiol. 38 (12), 1829–1840.
Nakatsuka, T., Sano, M., Li, Z., Xu, C., Tsushima, A., Shigeoka, Y., et al., 2020a. A 2600-year summer climate reconstruction in Central Japan by integrating tree-ring stable oxygen and hydrogen isotopes. Clim. Past 16 (6), 2153–2172.
Nakatsuka, T., Sano, M., Li, Z., Xu, C., Tsushima, A., Shigeoka, Y., 2020b. Reconstruction of Multi-millennial Summer Climate Variations in Central Japan by Integrating Tree-ring Cellulose Oxygen and Hydrogen Isotope Ratios.
Oerter, E., Finstad, K., Schaefer, J., Goldsmith, G.R., Dawson, T., Amundson, R., 2014. Oxygen isotope fractionation effects in soil water via interaction with cations (Mg, ca, K, Na) adsorbed to phyllosilicate clay minerals. J. Hydrol. 515, 1–9.
Oerter, E.J., Siebert, G., Bowling, D.R., Bowen, G., 2019. Soil water vapour isotopes identify missing water source for streamside trees. Ecohydrology 12 (4), e2083.
Pendall, E., 2000. Influence of precipitation seasonality on piñon pine cellulose δD values. Glob. Chang. Biol. 6 (3), 287–301.
Pflug, E.E., Siegwolf, R., Buchmann, N., Dobbertin, M., Kuster, T.M., Günthardt-Goerg, M.S., et al., 2015. Growth cessation uncouples isotopic signals in leaves and tree rings of drought-exposed oak trees. Tree Physiol. 35 (10), 1095–1105.
Pilcher, J.R., Frenzel, B., 1995. Biological considerations in the interpretation of stable isotope ratios in oak tree-rings. Problems of Stable Isotopes in Tree-rings, Lake Sediments and Peat-bogs as Climatic Evidence for the Holocene. S. 157 - 161, pp. 157–161.
R Core Team, 2020. R: a language and environment for statistical computing. Vienna, Austria. https://www.R-project.org/.
Reynolds-Henne, C.E., Saurer, M., Siegwolf, R.T.W., 2009. Temperature versus species-specific influences on the stable oxygen isotope ratio of tree rings. Trees 23 (4), 801–811.
Riechelmann, D.F.C., Greule, M., Siegwolf, R.T.W., Anhäuser, T., Esper, J., Keppler, F., 2017. Warm season precipitation signal in δ2H values of wood lignin methoxyl groups from high elevation larch trees in Switzerland. Rapid Commun. Mass Spectrom. 31 (19), 1589–1598.
Rinne, K.T., Loader, N.J., Switsur, V.R., Waterhouse, J.S., 2013. 400-year May–August precipitation reconstruction for southern England using oxygen isotopes in tree rings. Quat. Sci. Rev. 60, 13–25.
Roden, J.S., Ehleringer, J.R., 1999. Hydrogen and oxygen isotope ratios of tree-ring cellulose for riparian trees grown long-term under hydroponically controlled environments. Oecologia 121 (4), 467–477.
Roden, J.S., Ehleringer, J.R., 2000. Hydrogen and oxygen isotope ratios of tree ring cellulose for field-grown riparian trees. Oecologia 123 (4), 481–489.
Roden, J.S., Lin, G., Ehleringer, J.R., 2000. A mechanistic model for interpretation of hydrogen and oxygen isotope ratios in tree-ring cellulose. Geochim. Cosmochim. Acta 64 (1), 21–35.
Roden, J., Kahmen, A., Buchmann, N., Siegwolf, R., 2015. The enigma of effective path length for 18O enrichment in leaf water of conifers. Plant Cell Environ. 38 (12), 2551–2565.
Sachse, D., Billault, I., Bowen, G.J., Chikaraishi, Y., Dawson, T.E., Feakins, S.J., et al., 2012. Molecular paleohydrology: interpreting the hydrogen-isotopic composition of lipid biomarkers from photosynthesizing organisms. Annu. Rev. Earth Planet. Sci. 40 (1), 221–249.
Salmon, Y., Torres-Ruiz, J.M., Poyatos, R., Martinez-Vilalta, J., Meir, P., Cochard, H., et al., 2015. Balancing the risks of hydraulic failure and carbon starvation: a twig scale analysis in declining scots pine. Plant Cell Environ. 38 (12), 2575–2588.
Sanchez-Bragado, R., Serret, M.D., Marimon, R.M., Bort, J., Araus, J.L., 2019. The hydrogen isotope composition δ2H reflects plant performance. Plant Physiol. 180 (2), 793–812.
Sargeant, C.I., Singer, M.B., Vallet-Coulomb, C., 2019. Identification of source-water oxygen isotopes in trees toolkit (ISO-Tool) for deciphering historical water use by forest trees. Water Resour. Res. 55 (12), 10954–10975.
Sarris, D., Siegwolf, R., Körner, C., 2013. Inter- and intra-annual stable carbon and oxygen isotope signals in response to drought in Mediterranean pines. Agric. For. Meteorol. 168, 59–68.
Sauer, P.E., Schimmelmann, A., Sessions, A.L., Topalov, K., 2009. Simplified batch equilibration for D/H determination of non-exchangeable hydrogen in solid organic material. Rapid Commun. Mass Spectrom. 23 (7), 949–956.
Saurer, M., Siegenthaler, U., Schweingruber, F., 1995. The climate-carbon isotope relationship in tree rings and the significance of site conditions. Tellus B 47 (3), 320–330.
Saurer, M., Aellen, K., Siegwolf, R., 1997a. Correlating delta13C and delta18O in cellulose of trees. Plant Cell Environ. 20 (12), 1543–1550.
Saurer, M., Borella, S., Leuenberger, M., 1997b. δ18O of tree rings of beech (Fagus silvatica) as a record of δ18O of the growing season precipitation. Tellus B 49 (1), 80–92.
Saurer, M., Spahni, R., Frank, D.C., Joos, F., Leuenberger, M., Loader, N.J., et al., 2014. Spatial variability and temporal trends in water-use efficiency of european forests. Glob. Chang. Biol. 20 (12), 3700–3712.
Saurer, M., Kirdyanov, A.V., Prokushkin, A.S., Rinne, K.T., Siegwolf, R.T.W., 2016. The impact of an inverse climate-isotope relationship in soil water on the oxygen-isotope composition of Larix gmelinii in Siberia. New Phytol. 209 (3), 955–964.
Savard, M.M., 2010. Tree-ring stable isotopes and historical perspectives on pollution–an overview. Environ. Pollut. (Barking, Essex 1987) 158 (6), 2007–2013.
Schimmelmann, A., 1991. Determination of the concentration and stable isotopic composition of nonexchangeable hydrogen in organic matter. Anal. Chem. 63 (21), 2456–2459.
Shestakova, T.A., Martínez-Sancho, E., 2021. Stories hidden in tree rings: a review on the application of stable carbon isotopes to dendrosciences. Dendrochronologia 65, 125789.
Shestakova, T.A., Voltas, J., Saurer, M., Berninger, F., Esper, J., Andreu-Hayles, L., et al., 2019. Spatio-temporal patterns of tree growth as related to carbon isotope fractionation in european forests under changing climate. Glob. Ecol. Biogeogr. 28 (9), 1295–1309.
Simard, S., Giovannelli, A., Treydte, K., Traversi, M.L., King, G.M., Frank, D., et al., 2013. Intra-annual dynamics of non-structural carbohydrates in the cambium of mature conifer trees reflects radial growth demands. Tree Physiol. 33 (9), 913–923.
Song, X., Farquhar, G.D., Gessler, A., Barbour, M.M., 2014. Turnover time of the non-structural carbohydrate pool influences δ18O of leaf cellulose. Plant Cell Environ. 37 (11), 2500–2507.
Sprenger, M., Leistert, H., Gimbel, K., Weiler, M., 2016. Illuminating hydrological processes at the soil-vegetation-atmosphere interface with water stable isotopes. Rev. Geophys. 54 (3), 674–704.
Sternberg, L., Ellsworth, P.F.V., 2011. Divergent biochemical fractionation, not convergent temperature, explains cellulose oxygen isotope enrichment across latitudes. PLoS One 6 (11), e28040.
Szczepanek, M., Pazdur, A., Paweczyk, S., 2006. Hydrogen, carbon and oxygen isotopes in pine and oak tree rings from southern Poland as climatic indicators in years 1900–2003. Geochronometria 25, 67–76.
Tang, K., Feng, X., 2001. The effect of soil hydrology on the oxygen and hydrogen isotopic compositions of plants' source water. Earth Planet. Sci. Lett. 185 (3–4), 355–367.
Tang, K., Feng, X., Ettl, G.J., 2000. The variations in δD of tree rings and the implications for climatic reconstruction. Geochim. Cosmochim. Acta 64 (10), 1663–1673.
Thornthwaite, C.W., 1948. An approach toward a rational classification of climate. Geogr. Rev. 38 (1), 55.
Treydte, K., Frank, D., Esper, J., Andreu, L., Bednarz, Z., Berninger, F., et al., 2007. Signal strength and climate calibration of a european tree-ring isotope network. Geophys. Res. Lett. 34 (24).
Treydte, K., Boda, S., Graf Pannatier, E., Fonti, P., Frank, D., Ullrich, B., et al., 2014. Seasonal transfer of oxygen isotopes from precipitation and soil to the tree ring: source water versus needle water enrichment. New Phytol. 202 (3), 772–783.
Tyree, M.T., Cochard, H., 1996. Summer and winter embolism in oak: impact on water relations. Ann. For. Sci. 53 (2–3), 173–180.
Vicente-Serrano, S.M., Beguería, S., López-Moreno, J.I., 2010. A multiscalar drought index sensitive to global warming: the standardized precipitation evapotranspiration index. J. Clim. 23 (7), 1696–1718.
Vitali, V., Klesse, S., Weigt, R., Treydte, K., Frank, D., Saurer, M., et al., 2021. High-frequency stable isotop4e signals in uneven-aged forests as proxy for physiological responses to climate in Central Europe. Tree Physiol. 4 (11), 2046–2062.
Voelker, S.L., Brooks, J.R., Meinzer, F.C., Roden, J., Pazdur, A., Pawelczyk, S., et al., 2014. Reconstructing relative humidity from plant δ18O and δD as deuterium deviations from the global meteoric water line. Ecol. Appl. 24 (5), 960–975.
Wassenaar, L.I., Hobson, K.A., 2003. Comparative equilibration and online technique for determination of non-exchangeable hydrogen of keratins for use in animal migration studies. Isot. Environ. Health Stud. 39 (3), 211–217.
Wassenaar, L.I., Hobson, K.A., Sisti, L., 2015. An online temperature-controlled vacuum-equilibration preparation system for the measurement of δ2H values of non-exchangeable-H and of δ18O values in organic materials by isotope-ratio mass spectrometry. Rapid Commun. Mass Spectrom. 29 (5), 397–407.
Waterhouse, J.S., Switsur, V.R., Barker, A.C., Carter, A., Robertson, I., 2002. Oxygen and hydrogen isotope ratios in tree rings: how well do models predict observed values? Earth Planet. Sci. Lett. 201 (2), 421–430.
White, J.W., Cook, E.R., Lawrence, J.R., Wallace, S.B., 1985. The ratios of sap in trees: implications for water sources and tree ring ratios. Geochim. Cosmochim. Acta 49 (1), 237–246.
Wickham, H., 2016. ggplot2: Elegant Graphics for Data Analysis. Springer-Verlag, New York.
Yakir, D., DeNiro, M.J., 1990. Oxygen and hydrogen isotope fractionation during cellulose metabolism in Lemna gibba L. Plant Physiol. 93 (1), 325–332.
Zang, C., Biondi, F., 2015. Treeclim: an R package for the numerical calibration of proxy-climate relationships. Ecography 38 (4), 431–436.
Zapater, M., Hossann, C., Bréda, N., Bréchet, C., Bonal, D., Granier, A., 2011. Evidence of hydraulic lift in a young beech and oak mixed forest using 18O soil water labelling. Trees 25 (5), 885–894.
Zhao, L., Wang, L., Cernusak, L.A., Liu, X., Xiao, H., Zhou, M., et al., 2016. Significant difference in hydrogen isotope composition between xylem and tissue water in Populus euphratica. Plant Cell Environ. 39 (8), 1848–1857.
Zhou, Y., Grice, K., Chikaraishi, Y., Stuart-Williams, H., Farquhar, G.D., Ohkouchi, N., 2011. Temperature effect on leaf water deuterium enrichment and isotopic fractionation during leaf lipid biosynthesis: results from controlled growth of C3 and C4 land plants. Phytochemistry 72 (2–3), 207–213.
Zweifel, R., Rigling, A., Dobbertin, M., 2009. Species-specific stomatal response of trees to drought - a link to vegetation dynamics? J. Veg. Sci. 20 (3), 442–454.